Logging Amazon forest increased the severity and spread of fires during the 2015-2016 El Niño

Paulo Eduardo Barni [1]
Anelícia Cleide Martins Rego [2]
Francisco das Chagas Ferreira Silva [2]
Richard Anderson Silva Lopes [3]
Haron Abrahim Magalhães Xaud [4]
Maristela Ramalho Xaud [4]
Reinaldo Imbrozio Barbosa [5]
Philip Martin Fearnside [6,7] *

[1] Universidade Estadual de Roraima – UERR, *Campus* Rorainópolis
Av. Senador Helio Campos, s/nº, 69375-000, Rorainópolis, Roraima, Brazil.
pbarni@uerr.edu.br

[2] Universidade Estadual de Roraima – UERR, *Campus* Rorainópolis
Av. Senador Helio Campos, s/nº, 69375-000, Rorainópolis, Roraima, Brazil.
{anelycia.com@gmail.com; chagasferreirasilva@gmail.com}

[3] Corpo de Bombeiros Militares de Roraima, Coordenação Estadual de Proteção e Defesa Civil. Avenida Venezuela, 1271, 69309690 - Boa Vista, Roraima, Brazil. {raslopes@gmail.com}

[4] Empresa Brasileira de Pesquisa Agropecuária – Embrapa/RR. Rodovia BR 174, Km 8, Distrito Industrial. 69301-970, Boa Vista, Roraima, Brazil. {haron.xaud@embrapa.br; maristela.xaud@embrapa.br}

[5] Instituto Nacional de Pesquisas da Amazônia (INPA), Rua Coronel Pinto, 315. 69301-150. Boa Vista, Roraima, Brazil. reinaldo@inpa.gov.br

[6] Instituto Nacional de Pesquisas da Amazônia (INPA), Av. André Araújo, 2936. 69067-375, Manaus, Amazonas, Brazil. pmfearn@inpa.gov.br

[7] Brazilian Research Network on Global Climate Change – Rede Clima, Av. dos Astronautas, 1758 - Jardim da Granja, São José dos Campos - SP, 12227-010, Brazil
* Corresponding author

Logging Amazon forest increased the severity and spread of fires during the 2015-2016 El Niño

Abstract. Forest fires degrade Amazon forest and its natural functions. Logging, deforestation and the increased frequency of prolonged droughts have contributed to the high recurrence of forest fires in the Amazon. Fires have impacted areas that, until recently, were considered immune to fire, such as the southern portion of the Brazilian state of Roraima, which is characterized by forest types that occur in environments with high natural humidity but that are now strongly impacted by selective logging (SL). The objective of this study was to determine the severity and spread of fire in the forests of southern Roraima, taking as a reference the great forest fire that occurred during the 2015-2016 El Niño. We mapped fire scars and forest biomass from remote sensing and data from forest inventories in a 6657.3 km^2 study area, of which 6512.4 km^2 (97.8%) had originally been forest and 5412.3 km^2 (81.3%) was still forest in 2016. The 2015/2016 fires affected an estimated at 682.2 km^2, or 12.6% of the area that was still forest in 2016. Vulnerability maps of the forest were made using the weights-of-evidence method. The biomass impacted by fire totaled 26.4×10^6 Mg, representing 9.5% of the total mapped for the study area (277.4×10^6 Mg). The biomass killed by the fire totaled 5.8×10^6 Mg, representing 22.0% of the biomass affected by the fires. The highest level of fire severity (very strong) proportionally affected 84.6% more forest biomass inside than outside SL areas. Forest vulnerability to fires increased by 265.5% in terms of area and by 400.7% in terms of biomass when exposed to SL. Logging also increased the severity of fires when they occurred: a hectare of burned forest was 85.9% more likely to have a "very strong" fire if it had been previously logged, and burned areas that had been logged lost, on average, 2.9% more of their pre-fire biomass to the fire than those that had not been logged (86.5 Mg ha^{-1} versus 84.0 Mg ha^{-1}). Considering only the ombrophilous forest, the mean biomass of forest that was logged and burned was 310.7 Mg ha^{-1}, or 30.8% lower than the mean biomass of 448.7 Mg ha^{-1} in logged but unburned areas, showing a substantial biomass loss to fire (average of 138.0 Mg ha^{-1}). SL more than doubled the impact of fire on biomass loss as compared to the impact of the logging itself. In addition to its contribution to carbon emissions and other impacts, the amplifying effect of SL on forest fires indicates that the assumption that authorized forest management projects in Amazonia are sustainable is unwarranted. The future role of this practice should be rethought, existing projects should be subject to close inspection and control, and unauthorized logging should be identified and repressed. The policy of allowing sale of wood from clearcutting projects should be rethought because it provides a loophole for laundering wood from illegal logging.

Keywords: Environmental modeling; land use; land cover; Remote sensing; Amazon

1. Introduction

Forest fires are a threat to the integrity and biodiversity of forests (McLauchlan et al., 2020), and to the Amazon forest's carbon storage and hydrological cycling functions (da Silva et al., 2018; Fearnside, 2008; Fearnside et al., 2013; Rappaport et al., 2018; Ziccardi et al., 2019). The ignition sources of forest fires in the Amazon are

47 the result of human actions, such as burning in nearby newly cleared forest or for
48 pasture maintenance or for slash-and-burn family farming, while selective logging
49 plays an important role in making the forest vulnerable to the entry and propagation of
50 fire (Alencar et al., 2006; Aragão and Shimabukuro, 2010; Berenguer et al., 2014;
51 Brando et al., 2014, 2019; Uhl and Buschbacher, 1985; Xaud et al., 2013). SL has
52 been indicated as one of the factors for the spread of forest fires even in places that are
53 distant from the main foci of deforestation (Alencar et al., 2015; Broadbent et al.,
54 2008; Hethcoat et al., 2020; Silva et al., 2018).
55   Prolonged drought events driven by the increasing frequency of severe El Niño
56 events have a direct effect on the spread of forest fires in the Amazon (Aragão et al.,
57 2018; Jiménez-Muñhoz et al., 2016; Meira-Junior et al., 2020; Nepstad et al., 2004,
58 2007), as do the effects of changes in land use and cover and predatory logging
59 (Brando et al., 2014, 2019). The frequency of forest fires has increased in areas that
60 (until recently) were considered immune to fire due to the natural humidity of the
61 forest; however, the factors that attenuate or amplify fire occurrence are still little
62 studied (Barni et al., 2015a; da Silva et al., 2018; Fonseca et al., 2017; Turubanova et
63 al., 2018).
64   The Amazon provides essential environmental services (e.g., Fearnside, 2008),
65 and conserving these requires understanding of the interactions between climatic
66 phenomena and human activities and their effects on the degradation of forest
67 biomass. Systematic mapping is one of the remote-sensing tools of great importance
68 for the understanding the spatial distribution and the spreading behavior of forest fires
69 and it is an intelligent way to provide input for the improvement of public policies to
70 combat the indiscriminate use of fire. Systematic mapping can provide estimates of
71 greenhouse-gas (GHG) emissions on a large scale and contribute to improving the
72 calculations representing biomass and carbon affected by fire and deforestation
73 (Aragão et al., 2018; Baccini et al., 2012). Brazil's current National Inventory of GHG
74 Emissions (Brazil, MCTI, 2020) does not consider emissions from understory forest
75 fires when calculating emissions from land-use change and forestry. This fact persists,
76 in part, due to the small volume of work carried out in this area of knowledge and the
77 large uncertainties involved in calculating the emission factors.
78   Several spectral indices have been developed or adapted to improve the mapping
79 of burned areas: NDVI, SAVI, EVI, EVI2, GEMI, BAI, BAIM, NBR, NBR2, CSI and
80 MIRBI (Bastarrika et al., 2011; Chuvieco et al., 2002; Stropianna et al., 2012). New
81 approaches based on spectral mixture analysis (SMA) and image fractions (Quintano
82 et al., 2006) are useful for mapping burned areas. Canopy damage by selective logging
83 and fire, including their severity (capacity to damage the forest), have been
84 successfully mapped using the Normalized Difference Fraction Index (NDFI) (Souza
85 Jr. et al., 2005a, 2013).
86   Halting or greatly reducing deforestation would clearly have a substantial benefit
87 in avoiding forest fires because the burning of felled trees in newly cleared areas is a
88 major source of ignition for fire in adjacent forests. Note that the forest is not
89 intentionally set on fire, but rather fire escapes from nearby areas that are being burned
90 either as part of the initial clearing or in subsequent management of the agricultural
91 and ranching systems.
92   One of the great challenges we currently face is a better understanding of the
93 relationship between deforestation behavior and the application of efficient public

94   policies (West and Fearnside, 2021). Policies are also needed to help change the
95   practices used in agriculture and ranching (which today are still based on fire) to the
96   use of technologies that allow the incorporation into the soil of the biomass of second
97   growth cut to prepare forest for planting and in the maintenance of pastures free of
98   invading woody vegetation. However, implementation of these systems has proved to
99   be difficult in the Amazon because these alternatives to fire demand increased
100   production costs.
101   In the southern portion of Brazil's state of Roraima (in northern Amazonia),
102   deforestation is strongly stimulated by both legal and illegal logging (Barni et al.,
103   2020). In this region, authorizations to use wood from areas being deforested in
104   projects licensed for clearcutting by Roraima's State Foundation for the Environment
105   and Water Resources (FEMARH) provide the documentation for most of the "legal"
106   logs delivered to sawmills. However, much of the wood that theoretically comes from
107   the areas approved for clearcutting or for forest management does not actually come
108   from these areas, but rather from selective logging in forests that are not authorized for
109   either activity. For example, based on a questionnaire applied to 38% of the sawmills
110   in Rorainópolis in 2013, Crivelli et al. (2017) reported that 54% of the wood volume
111   came from deforestation projects, 11% from forest-management projects, and for 35%
112   of the wood the sawmill owners were "unable to specify" the source.
113   The great majority of requests to FEMARH from landowners for deforestation
114   authorizations are merely a means to legalize the sale of timber, rather than for the
115   stated purpose of clearing land for agriculture and pasture. This is clearly shown by
116   the fact that most of the 12,480.9 ha of deforestation authorized by FEMARH in
117   southern Roraima between 2010 and 2015, only 26.2% was actually deforested, as
118   shown by our mapping based on data from INPE's PRODES program (Brazil, INPE,
119   2020). If the authorized areas are, in fact, deforested, they are logged before the
120   deforestation is done; if these areas are not in fact deforested, the logging is done, and
121   the unharvested trees are left standing. The volume harvested in the authorized areas is
122   less than the authorized amount. It is reasonable to suppose that this is because, given
123   the lack of inspections, it is more profitable for the loggers to cut trees of the most-
124   valuable species in a wider area of forest than it is to harvest the permitted volume
125   only within the authorized area, where part of the harvest would be composed of less-
126   valuable species.
127   In January 2021 the municipality (county) of Rorainópolis (in southern Roraima)
128   was added to the federal "blacklist" of priority locations for actions to prevent,
129   monitor and control deforestation in the Amazon (Oliveira, 2021). Logging in this area
130   has only minimal control, and, due to insufficient staff, FEMARH, does not make field
131   inspections to verify that the specified limits and procedures are respected. The lack of
132   inspections at the sites undergoing logging or deforestation does not mean that all
133   parts of the production chain are free of influence from regulations. The federal
134   environmental agency (the Brazilian Institute for the Environment and Renewable
135   Natural Resources, or IBAMA) occasionally inspects sawmills to see if the amount of
136   wood present is compatible with the documentation. In 2018 such an inspection in
137   Rorainópolis found that virtually none of the sawmills were in compliance, and the
138   sawmills were shut down (G1, 2018a). Note that 2018 was after the 2015-2016 El
139   Niño fires that are the subject of the current study and was before the Jair Bolsonaro

140 presidential administration began in January 2019, with a notable relaxation of
141 environmental controls and gutting of IBAMA (see Ferrante and Fearnside, 2019).
142   Logging is not done by the owners of the land, but instead is done either by
143 logging teams working for sawmills or by independent loggers who pay a landowner
144 to allow the timber to be harvested and sold to sawmills. There is clearly no
145 motivation for sustainability, and those doing the logging may also invade adjacent
146 properties or government land to remove additional timber. Inspection is limited to
147 visits to sawmills to check if the volume of stockpiled wood is compatible with the
148 maximum amounts specified in the licenses. Logging trucks are occasionally stopped
149 by IBAMA to check the permit for transporting timber (the "document of forest
150 origin," or DOF), but if a truck is not stopped the transport permit is often reused
151 multiple times (Barni and Silva, 2017).
152   Throughout Brazilian Amazonia the permits issued for transporting timber from
153 authorized forest-management projects are frequently used in the same way as those
154 for deforestation projects, with the volume for which the permits are issued coming, in
155 reality, from logging in other areas, including indigenous lands and other protected
156 areas where logging is forbidden (Brancalion et al., 2018). Regardless of any official
157 authorization for "sustainable" forest management in rural properties in our study area,
158 the actual implementation of such practices was "null or incipient" at the time of our
159 study (Gimenez et al., 2015).
160   The present case study aims to determine the effects of SL on the severity and
161 spread of understory fire in southern Roraima considering the mega forest fire that
162 occurred in this part of the Amazon during the El Niño event of 2015-2016 (Fonseca
163 et al., 2017). Areas "affected" by forest fire are areas where an understory fire
164 occurred during the 2015-2016 El Niño as indicated by burned litter and charring at
165 the base of trees. Our hypothesis is that SL favored an increase in the severity of fire
166 and its spread (increased area affected by fire, both by the increased sizes of the fire
167 scars and by increased number of scars) both within the logged areas and in
168 neighboring unlogged areas, contributing to greater exposure of forest biomass to fire.
169 The specific questions the study addresses are: (i) What was the extent of the area
170 affected by fires and the amount of forest biomass lost in the study area considering
171 four levels of fire severity? (ii) What was the proportional contribution of SL in
172 spreading the fire? (iii) What was the area of the exposed forest and what was the
173 magnitude of forest biomass vulnerable to new forest fires in the study area?
174   To answer question (i) we used a geographic information system (GIS) and
175 geoprocessing tools, combined with inventory data, to assess the loss of forest biomass
176 at four levels of fire severity as defined by Fernandes-Manso et al. (2016) in areas with
177 signs of SL and in areas without signs of SL. To answer questions (ii) and (iii) we used
178 the weights-of-evidence method (Barni et al., 2015b, 2020; Soares-Filho et al., 2006;
179 Leite-Filho et al., 2021). Maps of weights-of-evidence have the ability to capture the
180 influence of variables that are spatially related to the occurrence of forest fire
181 (Silvestrini et al., 2011).
182   Our study will provide improvements for understanding the relationship between
183 the severity of fire and previous disturbance by SL. Among the uses for this
184 information is improvement of carbon-emission calculations due to forest degradation
185 in the Amazon (e.g., Brazil, MCTI, 2020).
186

2. Materials and Methods
2.1 Study area

The study area is located in the southern portion of the state of Roraima, covering the areas that include the seat of the municipality (county) of Rorainópolis and the towns (*vilas*) of Colina and Equador. The area also includes small parts of the municipalities of Caracaraí (90.5 km^2, 1.4% of the study area) and São Luiz (164.2 km^2, 2.5%) (Table S1 in the Supplementary Material). The area includes 130.6 km of Highway BR-174 and 1249.4 km of secondary roads in the settlement projects and their surroundings (Figure 1). The study area, which comprises 6657.3 km^2, was delimited by clipping a Landsat 8 image for 9 June 2016 (row 231, path 60) and intersecting it with part of scenes 20NQG and 20NQF of the vector grid of the Sentinel-2 satellite (https://www.instrutorgis.com.br/download-da-grade-do-satelite-sentinel2/). The vegetation cover is composed of dense rain forest (in its vast majority), in addition to mosaics of *campinarana* (oligotrophic woody vegetation) and ecotone areas between *campinarana* and dense rain forest (Barni et al., 2016). Under the Köppen classification system, the region's climate is *Af* (equatorial forest climate) (Alvares et al., 2014).
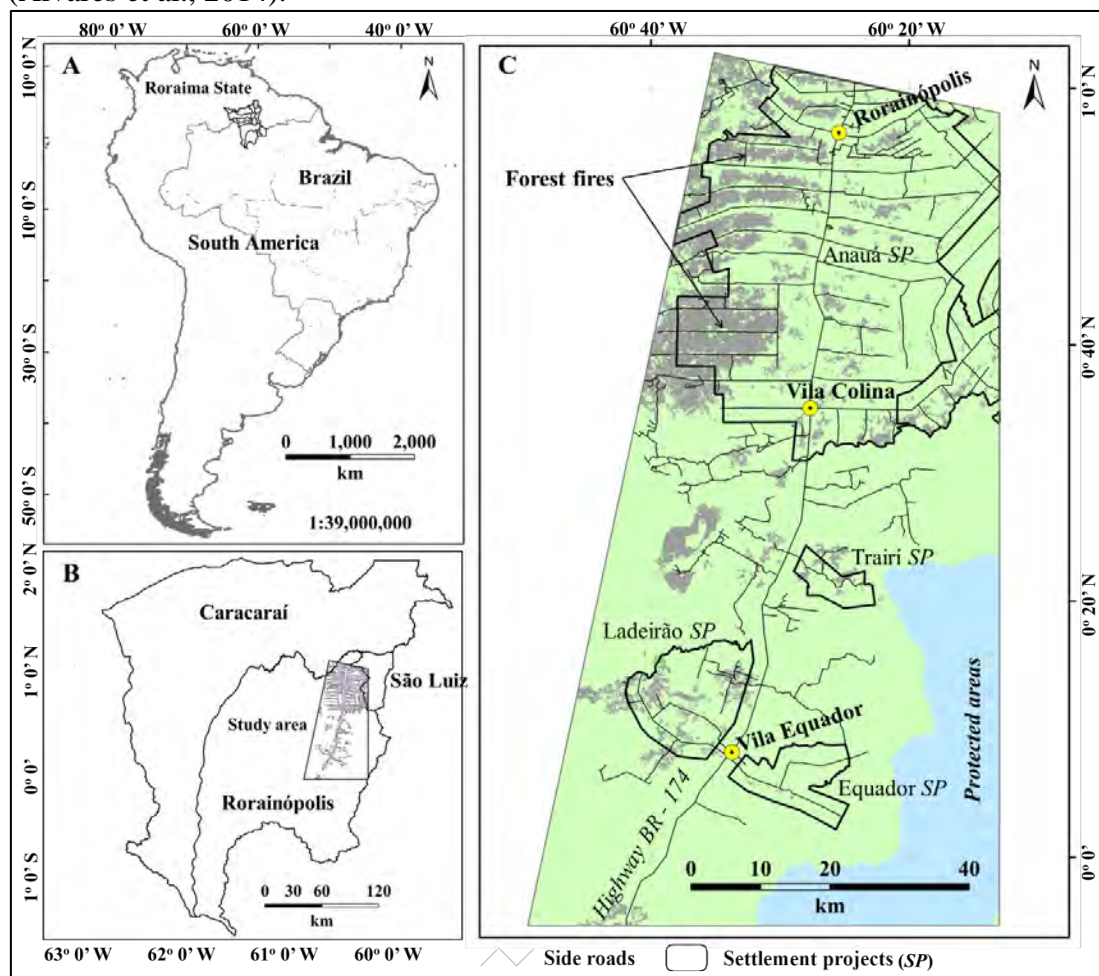
Figure 1. (A) Map of South America showing the state of Roraima. (B) Municipalities and the location of the study area. (C) Detailed map of the study area.

208 **2.2 Databases**

209   The database consisted of 1.) A vector grid from the Sentinel-2 satellite (which
210 was used to delimit the study area), 2.) Landsat 5 and 8 images from 2010 to 2016 for
211 path/row 231/60, obtained from the US Geological Survey (USGS, 2016) (which were
212 used to map the dynamics of SL and fire) 3.) A Shuttle Radar Topography Mission
213 (SRTM) image (USGS, 2016) (which served to represent the altitude and the slope in
214 the study area), 4.) A vector map of forest types (Brazil, PROBIO, 2013), 5.) A map of
215 deforestation and non-forest obtained from PRODES (Brazil, INPE, 2020), 6.) A
216 vector map of forest fires (Barni et al., 2017) (used to represent the burned area), 7). A
217 map of total forest biomass (live + dead and above + belowground) in Roraima (Barni
218 et al., 2016) (used to estimate biomass loss and affect by fire), 8.) Vector maps of
219 roads and rivers, 9.) A vector map of hot spots between 1 December 2015 and 23
220 March 2016 from the AQUA-MT reference satellite
221 (http://queimadas.dgi.inpe.br/queimadas/bdqueimadas/) (used to represent the initial
222 scenario of fires in the study area using the weights-of-evidence method), 10.) Forest
223 inventory data on observed fire and tree mortality in 17 transects measuring 4×250 m
224 (1.7 ha) at the locations of fires that occurred in the study area during the 2015/2016
225 El Niño event (Table S2) (used to estimate the biomass loss at the plot level).

226   For the processing of variables (maps), analyses were performed using the
227 Quantum Gis (QGis) Desktop 2.18.15 (https://www.qgis.org/) geographical
228 information system (GIS). Maps 2 to 9 (except map 7) and products derived from
229 these have been used for analyzes with the weights-of-evidence method (Barni et al.,
230 2015b, 2020; Soares-Filho et al., 2006; Leite-Filho et al., 2021) in Dinamica-EGO 5.0
231 software (https://csr.ufmg.br/dinamica/). Statistical analyses were performed using R
232 version 3.6.0 software (https://www.r-project.org/).
233   The database included information on authorizations for logging (authorized area
234 in ha and volume in m^3) in the area licensed for "alternative land use" (deforestation)
235 from 2010 to 2015 (Table S3); the database also included information on "Sustainable
236 Forest Management Plans" from 2017 to 2020 (Table S4), which were used to support
237 the analyses. These data were provided by the State Foundation for the Environment
238 and Water Resources (FEMARH) under the technical collaboration agreement
239 001/2020 between FEMARH and the State University of Roraima (UERR). The
240 methodological sequence for obtaining and analyzing the data followed the flowchart
241 in Figure 2.
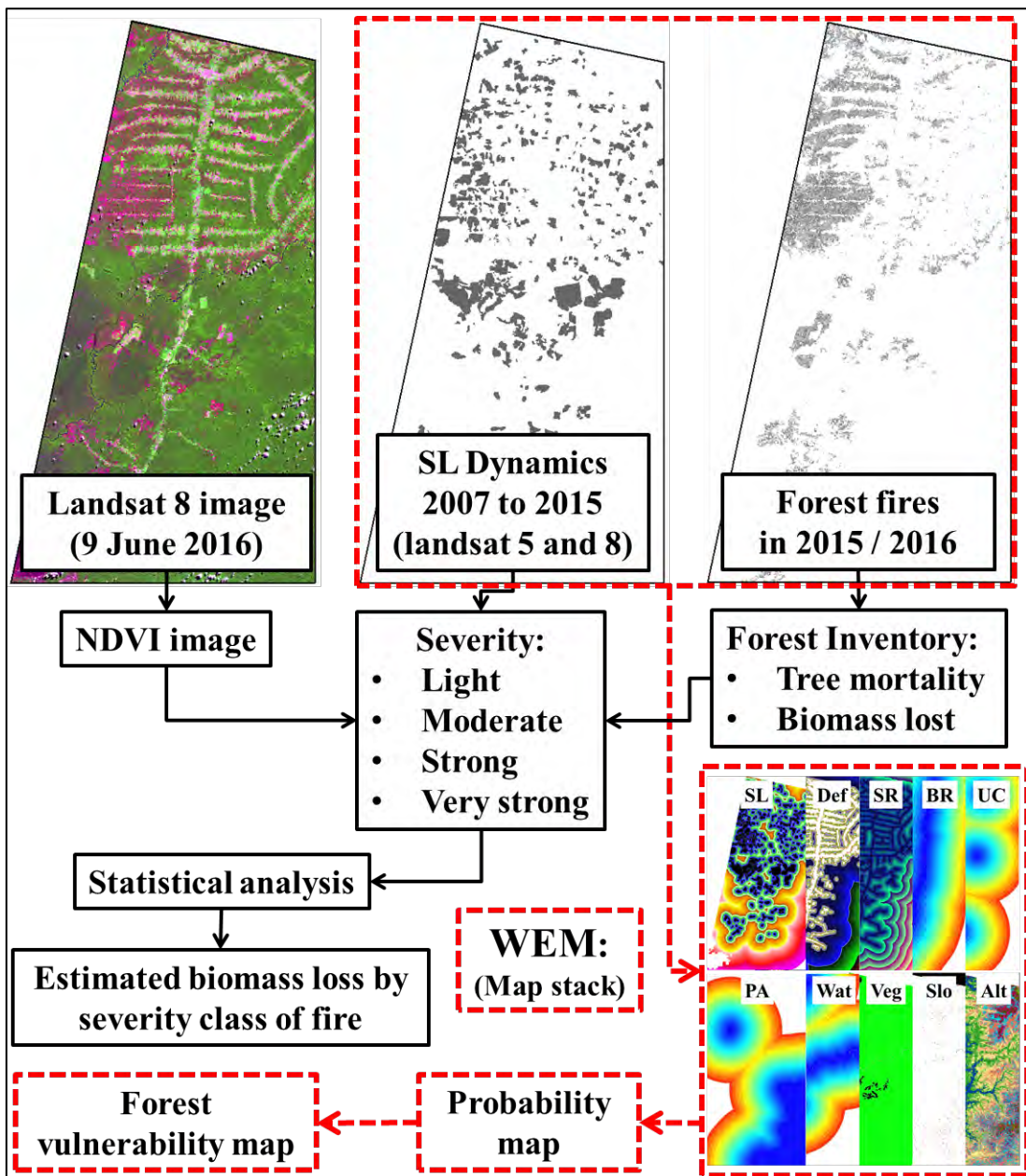
Figure 2. Flowchart of the methodology applied in the study area to obtain and analyze the data. SL = selective logging; NDVI = normalized difference vegetation index. WEM = weights-of-evidence method. Continuous variables (distance map): SL = selective logging, Def= deforestation, SR = secondary roads, BR = BR – 174 highway, UC = urban centers, PA = protected area and Wat = water. Categorical variables: Veg = vegetation, Slo = slope and Alt = altitude.

2.3 Methods
2.3.1 Fire severity

Assessment of the severity of the fire consuming the combustible material and killing a fraction of the living forest biomass above and below ground was conducted according to the technique recommended by Fernándes-Manso et al. (2016), using vegetation indices, including the normalized difference vegetation index (NDVI). In

256 this approach, the NDVI values were extracted from the Landsat 8 image for 9 June
257 2016 (231/60) corresponding to the burned forest in the study area, and discrimination
258 was made among four increasing levels of fire severity: light, moderate, strong and
259 very strong (Table 1). The break points of the classification intervals for NDVI values
260 were set automatically by the software (Jenks natural breaks: Dent, 1990; Slocum,
261 1999) in five classes, with the fifth class (-1 to 0.2246) corresponding to pixels with
262 spurious values, which were excluded from the analysis. In the study by Fernándes-
263 Manso et al. (2016), based on visual interpretation of images from the Pleiades-1A/1B
264 sensor, the 'light' class corresponded to minor or insignificant damage from the fire
265 scar; the 'moderate' class corresponded to a moderately damaged area; the 'strong'
266 severity level corresponded to a highly damaged area and; the 'very strong' severity
267 level corresponded to an area totally destroyed by fire. Although the study by
268 Fernandes-Manso et al. (2016) was carried out in a region of Spain dominated by
269 *Pinus pinaster* Ait and *Quercus pyrenaica* Wild, which is a type of a vegetation
270 completely different from that in the Amazon, it is important to highlight that in our
271 study we only used the nomenclature for fire-severity classes based on these authors,
272 corresponding to the classes for separation of the NDVI values obtained in our study
273 area. Our choice was based on the familiarity with the use of NDVI and the evaluation
274 of various vegetation indexes carried out by Fernandes-Manso et al. (2016). These
275 authors indicated that the NDVI achieved scores similar to that of the normalized burn
276 ratio (NBR) in a Cox and Snell pseudo-R^2 test (0.430 and 0.450) and in a McFadden
277 pseudo-R^2 test (0.289 and 0.247) for NDVI and NBR respectively. In our study, NDVI
278 was highly correlated with NBR (Figure S1 and S2; Table S5).
279
280 **Table 1**. Increasing levels of fire severity observed in the study area.

Level	Class	NDVI (this study)	* NDVI
0	Light	0.4082 to 0.6031	0.5840 to 0.6195
1	Moderate	0.3641 to 0.4081	0.5225 to 0.5700
2	Strong	0.3140 to 0.3640	0.4095 to 0.4495
3	Very strong	0.2247 to 0.3139	0.2267 to 0.2637

281 * Values estimated from Fernándes-Manso et al. (2016).
282
283 **2.3.2 Estimation of biomass loss by fire-severity class**
284   We used tree mortality or biomass-loss levels (inventory data) to numerically
285 define these classes and associate them with the corresponding severity levels. To
286 estimate biomass loss by fire-severity class, we used loss fractions of forest biomass
287 (Mg ha^{-1}) derived from the database for the forest inventory in the 17 transects (4 ×
288 250 m: 1.7 ha) carried out between 11 March and 6 April 2016 for trees with DBH ≥
289 10 cm. In the 17 plots (14 plots with SL and three plots without SL), 1180 individuals
290 (694 individuals ha^{-1}) were inventoried, of which 239 individuals (20.3%) had been
291 killed by fire. Trees that were considered to have been "killed" were observed in the
292 field (1-3 months after the fires) and judged to be dead based on lack of leaves,
293 appearance of the bark and signs of severe damage from the fire. The percentages for
294 estimating biomass loss in trees with DBH ≥ 10 cm were derived from the forest-
295 inventory data. The 10.4% loss percentage represented by the aboveground dead
296 biomass (litter) and the 2.4% aboveground biomass loss in dead trees with DBH < 10
297 cm were derived from the study by Barbosa and Fearnside (1999) (Table 2).

298
299 **Table 2.** Fractions of biomass loss from fire used in the GIS raster calculator for calculations
300 of biomass loss by fire severity class.

Severity	Litter	DBH <10 cm	DBH ≥10 cm	Loss fraction
Light	0.104	0.024	0.022	0.150
Moderate	0.104	0.024	0.074	0.202
Strong	0.104	0.024	0.151	0.279
Very strong	0.104	0.024	0.329	0.457

301
302   The volume is converted to biomass using the average basic density of 0.770 of
303 the 11 species that contributed the most wood volume to nine sawmills surveyed in
304 2013 in Rorainópolis by Crivelli et al. (2017), based on basic density values from
305 Fearnside (1997), Nogueira et al. (2005) and Silveira et al. (2013), weighted by their
306 respective percentages of the volume processed by the sawmills (Table S6). "Basic
307 density" of wood is oven-dried mass divided by saturated volume. A calculation is
308 made of the biomass removed in the harvested logs, together with the loss of
309 aboveground live biomass in the crowns and stumps of the harvested trees and in
310 collateral damage to unharvested trees caused by the logging operations
311 (Supplementary Material, Section 1.7: Table S7). The biomass lost (35.67 Mg ha^{-1}),
312 when divided by the average total biomass value (435.3 Mg ha^{-1}) of the dense
313 ombrophilous forest in the study area (Barni et al., 2016), results in a loss fraction of
314 0.082. In this approach it is assumed that the SL had already been removed this
315 fraction of the biomass, and the fraction is therefore applied as a constant regardless of
316 the fire-severity class.
317   To derive these loss percentages and assign the biomass values corresponding to
318 each severity class, the DBH ≥ 10 cm information on the inventoried trees (1180
319 individuals) was converted into aboveground dry biomass according to the model ln
320 (P) = β0 + β1 ln (DBH) + ε, proposed by Higuchi et al. (1998), where P is the fresh
321 weight (kg^{-1}) of the biomass, β0 (-1.497) and β1 (2.548) represent the regression
322 parameters (intercept and slope), ln is the natural logarithm and ε is the random error.
323 Values for fresh biomass (kg ha^{-1}) were converted to dry biomass (Mg ha^{-1}) based on
324 the mean water content of 40% found by Higuchi et al. (1998) (Table S2).
325   In order to represent the fire-damage classes overlapping the inventory transects, a
326 15-m buffer was created around the length of each transect. Next, the fire-severity
327 class values were extracted from a raster file intersecting the buffer areas (Figure 3A);
328 the average percentages were attributed for the biomass loss corresponding to each
329 class indicated in the pixels, which were estimated by the model, and the total biomass
330 was calculated for the 17 transects (Figure 3B).
331
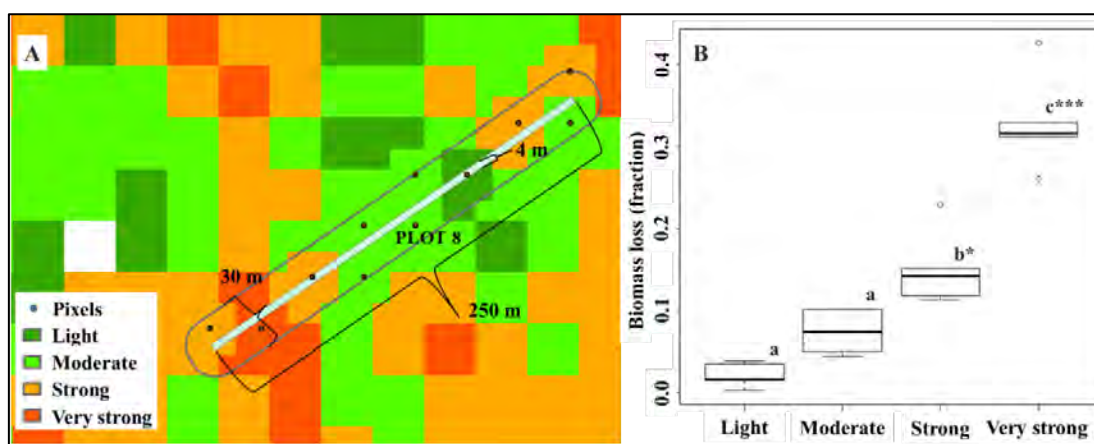
Figure 3. (A) Levels of fire severity along a plot inventoried in the field and (B) corresponding rates (fractions) of biomass loss. Equal letters = not significant; * = significant at 5%; *** = significant at 0.1% statistical probability.

2.3.3 Biomass of fire-affected areas by forest type

The biomass (Mg ha^{-1}) affected by the fires in each vegetation type was calculated using the biomass map prepared by Barni et al. (2016) in a grid-cell (raster) format. This biomass estimate was based on bole volumes of individual trees ≥ 31.8 cm DBH surveyed by the RADAMBRASIL project (Brazil, RADAMBRASIL, 1973-1983) in 298 1-ha plots (of which 119 were in Roraima and the remainder within 100 km of the state's borders). Volumes were converted dry biomass based on the wood basic density by species from Fearnside (1997), and adjustments for crowns, small trees, hollow trees, irregular trunks and other components were based on Nogueira et al. (2008).

Initially the biomass map was intersected with the forest-typology map, also in raster format, and the study area was cut out. The study area contained three vegetation types: Dense ombrophilous forest (DS), *Campinarana* (Ld) and Ecotones (LO). Note: the two-letter vegetation codes are those used by the Brazilian Institute for Geography and Statistics (IBGE). The biomass map for the study area was intersected with the forest-fire raster map (value=1). These map-algebra operations were performed using the raster calculator in the GIS. The same procedure was carried out to calculate the biomass loss caused by deforestation up to 2016 (Brazil, INPE, 2020).

2.3.4 Characterization of selective logging in the study area

To characterize SL in terms of the area that was logged and affected by understory forest fires in the entire study area, a systematic mapping of timber activity in the region was carried out between 2007 and 2015 using 16 satellite images (path/row 231/59 and 231/60) from Landsat 5 (2007 to 2011) and Landsat 8 (from 2013 to 2015) (Table S8 and Figure S3). For this purpose, RGB and NDVI images were interpreted visually, proceeding to manual editing in vector files of the SL areas in each image, as in Barni et al. (2015a) (Supplementary material: Section 1.8). As a way of assessing the influence of SL on the spread of fire and on the severity classes in the study area, tests were carried out to compare the NDVI values from 2016 with the NDVI values of the images from 2010, 2013, 2014 and 2015 at the same geographical coordinates in

367 areas affected by fires and with a history of SL. Additionally, analyses of fire severity
368 were carried out according to the year of selective logging occurrence (Table S9).
369
370 **2.3.5 Fire-vulnerability map with weights-of-evidence method**

371   The map of the forest's vulnerability to fire was obtained from the calculation of
372 the transition-probability map using the weights-of-evidence method (Supplementary
373 material: Figures S4, S5 and S6). This method stores information as numerical values
374 that are spatially referenced (x and y coordinates) representing the contribution
375 (evidence) of each variable in favoring or inhibiting the occurrence of the event under
376 study (in our case, fire), based on the occurrence of this event in the past. In other
377 words, the weights-of-evidence method has the ability to capture the influence of a set
378 of variables related to the spatial occurrence of a given event in the past and use that
379 evidence (weights-of-evidence coefficients) to build a spatial-probability map for the
380 occurrence of the event in question. This ability has often been exploited in simulating
381 future deforestation and forest-fire scenarios in the Amazon (Barni et al., 2015b, 2020;
382 Leite-Filho et al., 2021; Silvestrini et al., 2011; Soares-Filho et al., 2006).
383   For the preparation of the vulnerability map of the forest to understory forest fires,
384 a methodological sequence was used that involved the preparation of initial and final
385 scenario maps in Dinamica-EGO software. First, a land-use map was prepared with
386 the value classes (1) Deforested, (2) Forest and (3) Fire. The latter consists of 216 hot
387 spots detected in the study area by the AQUA-MT satellite between 1 December 2015
388 and 23 March 2016 (the time window when fire occurrences intensified in the study
389 area), transformed into pixels, representing the fire class (value=3) before the spread
390 of the fire (initial scenario). Second, a land-use map was prepared with the same
391 classes, but with the fire class applied to all of the fire spread detected in the study area
392 in 2016 (final scenario), which was obtained from the mapping carried out by Barni et
393 al. (2017) (Figure 4).
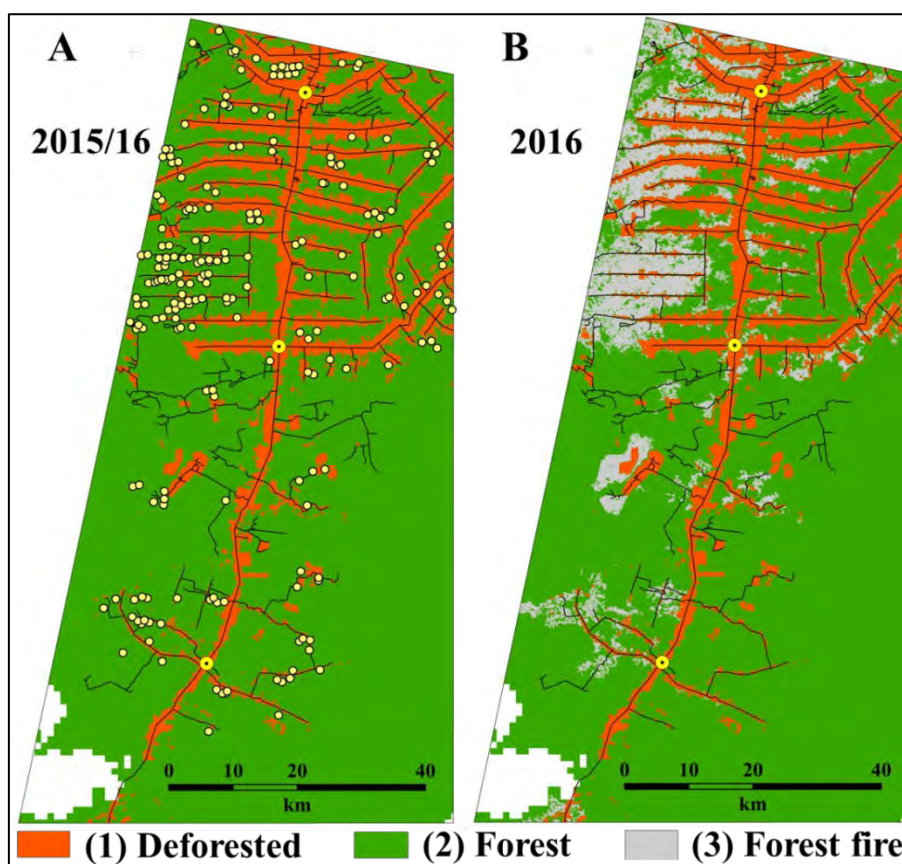
394
395 **Figure 4.** Input scenarios for the method of calculating the weights-of-evidence using
396 Dinamica-EGO software. (A) 2015-2016 Scenario (initial map) prepared with hot spots
397 between 1 December 2015 and 23 March 2016. (B) Scenario in 2016 (final map) after the
398 occurrence of fires in the region.
399

400   Twelve maps were created with the same number of columns and rows. Seven of
401 the maps were for environmental variables: (1) forest (vegetation), (2) deforestation,
402 (3) fire, (4) SL, (5) SL class year (area of polygons of SL mapped each year), (6)
403 hydrography (water courses), (7) relief and (8) slope. Four maps were for
404 infrastructure: (9) urban centers, (10) secondary roads, (11) BR-174 and (12) protected
405 areas (Indigenous Lands + conservation units). This step also involves the creation of
406 maps of distance-intervals (ranges) to fire scars for eight continuous variables and
407 creation of class intervals for the other four variables (vegetation, altitude, slope and
408 SL class year), which are considered to be categorical. The mapped variables (as a
409 data stack) served as inputs for calculating the weights-of-evidence coefficients
410 (Figures S3 and S4) using Dinamica-EGO software.
411   In addition to these initial procedures, a transition matrix was also calculated,
412 which is an array of the rates that the software uses to perform the transitions of pixels
413 between states. For example, a pixel representing forest (value=2) at time t_1 can
414 convert to a pixel representing fire (value=3) at time t_2, in a simulated scenario. In the
415 simulation model, the transition matrix provides the number of pixels that are ready
416 for the change of state, while the transition probability map directs the change to the
417 areas of greatest probability.

418   Correlation tests were performed to determine the association between variables
419   and to assess their spatial dependence (Bonham-Carter, 1994). Correlations with a
420   value of r ≥ 0.5 were considered to represent a strong association between the
421   variables (Cohen, 1988). These steps were performed using Dinamica-EGO software
422   (Supplementary Material).
423
424   **2.3.5.1 Assessment of the effect of SL on fire spread**

425   It is important to note that fire-severity classes were not considered in assessing
426   the effect of SL on the spread of fire in the forest. To assess fire spread we considered
427   five vulnerability classes that were calculated and mapped using the weights-of-
428   evidence method. The following procedures were performed to test the effect of SL on
429   the spread of fire in the study area: 1.) making a transition-probability map using all of
430   the variables in the database; 2.) making a transition-probability map using all of the
431   database variables except for the SL variable; 3.) making a transition-probability map
432   using only database variables with little or no correlation with SL and SL class year
433   and; 4.) making a transition-probability map using only SL and SL class year together
434   with the database variables with little or no correlation with SL. These procedures
435   were also carried out for the variables "deforestation" and "secondary roads," which
436   were highly correlated with SL in the study area (Table S10). The sizes (km^2) of five
437   classes of vulnerability of the forest to fire were then compared on the maps. The
438   difference (in %) in the size of the area of the class with the greatest vulnerability to
439   fire was calculated by comparing the map made using the set of variables that included
440   both SL and the variables without correlation with SL with the probability map
441   calculated only with the set of variables without correlation with SL. The percentage
442   difference was considered to represent the effect of SL on the spread of fire in the
443   study area. For the purpose of comparison and to serve as a reference in order to
444   support the discussions, the same procedure described above was performed for the
445   variables "deforestation" and "secondary roads." The effects of the variables were also
446   expressed in terms of biomass (Mg) vulnerable to fire in the study area. In this case,
447   only the area in the class with the highest probability of fire was considered for the
448   purpose of applying the biomass calculations in making the comparison between the
449   models.

450
451   **2.3.6 Validation of models**

452   To validate the simulation models, the reciprocal-similarity comparison technique
453   was used (Soares-Filho et al., 2008) based on adaptation of the fuzzy-similarity
454   method and the Kfuzzy method, which is considered to be equivalent to the Kappa
455   statistic and takes into account the fuzziness of both location and category within a cell
456   neighborhood (Hagen, 2003). The method is based on the state of the central cell of
457   each window, observing the similar and divergent states of the cells in its
458   neighborhood (or proximity) as a parameter of comparison between the maps. In this
459   approach, the simulated fire scenario is compared with the 2015-2016 scenario (initial
460   scenario) and with the 2016 scenario (map of fire that actually occurred) using
461   "windows" of different sizes in an exponential decay function (truncated outside of a
462   window size of 11 × 11 cells) (Figure S7). The exponential decay function records the
463   scores of the comparisons between maps produced with increasing window sizes (3 ×

464 3 pixels, 5×5 pixels, …, 11×11 pixels), and the test result (%) is returned as a .csv
465 table file (Figure S7). The window acts as a filter covering all of the lines in the raster
466 map to make the comparison (Figure S7). Models are generally considered to be valid
467 for simulation when the similarity value for the maps being compared is $\geq 50\%$ (Barni
468 et al., 2015b, 2020). The tests were carried out in a sub-model of the Dinamica-EGO
469 software (Figure S8).
470
471 **3. Results**
472 **3.1 Areas of occurrence**

473 The area of understory forest fires that occurred in our study area during the 2015-
474 2016 El Niño event totaled 682.2 km^2, affecting 12.6% of the remaining original
475 forest. The cumulative deforestation in 2016 (observed since the 1970s and 1980s) in
476 this region (1102.1 km^2) represented 16.6% of the study area and 16.9% of the area
477 that was originally forest (Table S11). The cumulative deforestation attributed to the
478 portion of the municipality of Rorainópolis located within the study area represented
479 90.8% of the deforestation observed in the entire municipality up to 2016 (1151.2 km^2:
480 Brazil, INPE, 2020) (Table S1).
481 In the study area, SL mapped between 2007 and 2015 totaled 644.8 km^2. Of this
482 SL area, 28.0% (180.7 km^2) was also affected by understory forest fire (Table S11 and
483 Figure S3).

484 **3.2 Estimation of biomass in areas affected by forest fires**

485 The largest amount of biomass affected by the fires (22.7×10^6 Mg) was under
486 ombrophilous forest (dense rain forest) and the smallest (0.3×10^6 Mg) was found in
487 ecotone forests (Table S12). The fire scars spread along the BR-174 and its secondary
488 roads from the vicinity of the Rorainópolis municipal seat to an area near Vila
489 Equador (Figure 1).
490 The total biomass affected by fires in our study area was estimated at 26.2×10^6
491 Mg, while the biomass affected by fires in the SL area was estimated at 6.7×10^6 Mg
492 (Table S12). This represents 24.1% of the total biomass in areas subjected to SL,
493 estimated at 27.9×10^6 Mg. Estimation of forest biomass was performed for each
494 forest type, separating areas of SL and areas without SL are presented in Table S13.
495 Estimates of biomass loss from deforestation until 2016 are presented in Table S14 for
496 in the study area as a whole and separately for each forest type.
497
498 **3.3 Fire-severity gradient area**

499 The most widespread severity level in the study area was the light-intensity class
500 (36.2%), considering areas burned without SL. When considering the same severity
501 level but in areas with SL, the light-intensity class decreased by 27.9% in relation to
502 the area without SL. On the other hand, when considering the highest level of fire
503 severity (very strong) the area under SL shows an increase of 85.9% in terms of
504 incident area of this class in relation to the area without SL (Table 3). This means that,
505 if a hectare of forest burns, it is 85.9% more likely to be a very-strong burn if that
506 hectare had been previously logged.
507

508
509 **Table 3.** Area of severity classes of understory fire without selective logging and with.

Severity	Total Area (km²)	%	Wo/SL Area (km²)	%	W/SL Area (km²)	%	Difference with SL%
Light	246.5	36.2	195.5	39.1	51.0	28.2	-27.9
Moderate	229.0	33.5	170.6	34.0	58.3	32.3	-5.3
Strong	140.7	20.7	95.5	19.1	45.2	25.0	31.2
Very strong	64.9	9.6	38.8	7.8	26.1	14.5	85.9
Total	**681.1**	**100**	**500.4**	**73.5**	**180.7**	**26.5**	–

510 W/SL = with selective logging. Wo/SL = without selective logging.
511

3.4 Vulnerability of the forest to understory fires in SL areas

513   The assessment of the vulnerability maps showed that SL influenced the spread of
514 fire in the study area during the 2015/2016 El Niño event within the fire-severity
515 classes. Analyses of NDVI images show a positive correlation between fires and the
516 logging carried out in years immediately prior to the fires. On the other hand, this
517 effect was not observed when comparing the NDVI values of the images of locations
518 that had been subjected to SL in 2010 with the NDVI values obtained in the same
519 places after the 2015/2016 fires (Figure S9).
520   These results are confirmed by annual SL data from satellite images (Table S8)
521 and analysis of the distances from the edge of the forest to the locations of the fires
522 and the SL. The largest fire recorded in areas affected by SL (161.2 km²) occurred in
523 the distance range from 0 to 1200 m, representing 89.3% of the total spread of fire
524 (180.5 km²) in the area with SL. The years that contributed most to the area of SL
525 were 2013, 2014 and 2015, providing the SL-disturbed area through which the fires
526 crossed and spread to neighboring areas (Figure 5A). Beginning in 2011 there is a
527 strong inversion of the severity classes, with locations with more-recent SL burning
528 with greater severity in the 2015/2016 fires (Figure 5B, Table S9).
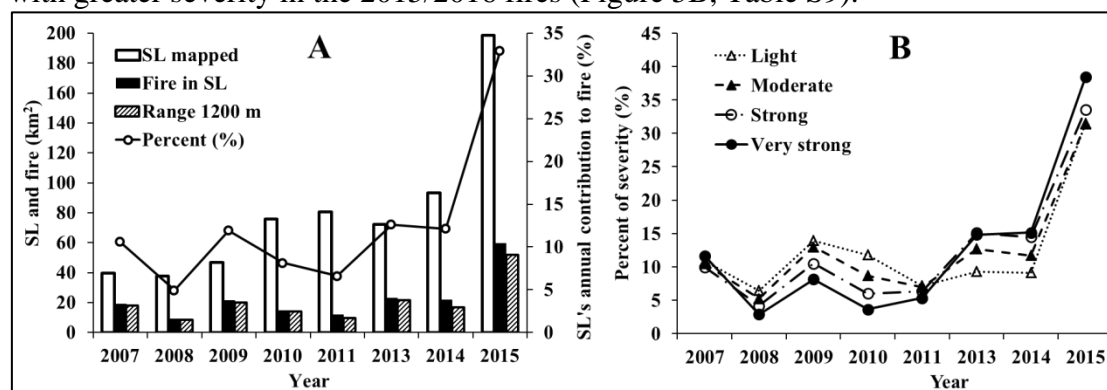
529
530 **Figure 5**. (A) Annual contribution of areas impacted by SL that were burned during the
531 2015/2016 El Niño event in the study area. (B) Gradient of fire severity depending on the year
532 of logging.
533

3.5 Estimation of biomass loss by fire-severity class

535   The biomass affected by forest fires totaled 26.4×10^6 Mg (Table 4), with the
536 biomass in the fire-affected SL areas totaling 6.7×10^6 Mg (25.4 of the fire-affected

537 biomass), while the biomass computed outside of the SL areas represented 74.6%. The
538 highest severity level ("very strong") affected, proportionally, 84.6% (14.4 versus 7.8)
539 more biomass in SL areas than outside of these areas (Table 4).

540 **Table 4.** Estimated biomass affected by fire for each fire-severity class considering all forest
541 types.
542

Severity	Area (km²)	Wo/SL (10⁶ Mg)	% of biomass	Area (km²)	W/SL (10⁶ Mg)	% of biomass	SL (10⁶ Mg)	% of biomass	Total (10⁶ Mg)
Light	195.5	7.5	38.1	51.1	1.9	28.2	0.17	28.3	9.4
Moderate	170.6	6.8	34.6	58.3	2.2	32.3	0.19	32.4	9.0
Strong	95.5	3.9	19.5	45.2	1.7	25.2	0.15	25.2	5.6
Very strong	38.8	1.5	7.8	26.1	1.0	14.4	0.09	14.4	2.5
Total	**500.4**	**19.8**	**100.0**	**180.7**	**6.7**	**100.0**	**0.6**	**100.0**	**26.4**

543 W/SL = with selective logging. Wo/SL = without selective logging.
544

545   The largest amount of biomass killed by fires (1.8×10^6 Mg; mean 79.1 Mg ha^{-1})
546 was in the "moderate-loss" class, representing 30.8% of the total estimated biomass.
547 The smallest amount of biomass (1.1×10^6 Mg; mean 176.3 Mg ha^{-1}) was in the class
548 with the highest fire severity, representing 19.5% of the total biomass killed by the
549 fires. Considering the level of greatest severity, the loss in the SL areas was,
550 proportionally, 68.3% greater than in the areas without SL (27.6% versus 16.4%,
551 respectively) (Table 5
552

553
554 **Table 5.** Estimation of biomass killed by fire for each fire-severity class considering all forest
555 types.

Severity	Wo/SL			W/SL			Total		
	Biomass (10⁶ Mg)	%	Mean (Mg ha⁻¹)	Biomass (10⁶ Mg)	%	Mean (Mg ha⁻¹)	Biomass (10⁶ Mg)	%	Mean (Mg ha⁻¹)
Light	1.1	26.5	58.1	0.3	17.8	55.7	1.4	24.2	57.6
Moderate	1.4	32.0	80.3	0.4	27.5	75.5	1.8	30.8	79.1
Strong	1.1	25.0	111.8	0.5	29.5	104.6	1.5	26.2	109.5
Very strong	0.7	16.4	181.1	0.4	27.6	169.3	1.1	19.5	176.3
Dead	**4.3**	**21.7**	**84.1**	**1.6**	**23.9**	**92.6**	**5.9**	**22.3**	**86.4**
Affected	**19.7**	**7.9**	–	**6.7**	**24.3**	–	**26.4**	**9.5**	**387.6**
Total	**249.8**	**90.1**	–	**27.6**	**9.9**	–	**277.4**	**100.0**	–

556
557 W/SL = with selective logging. Wo/SL = without selective logging.
558

559   An increase in biomass loss with increasing fire severity is apparent, and the loss
560 is greater at each intensity of fire if the area had been subjected to SL. If one considers
561 only omprophilous forest, which represents 78.1% of the area affected by fire and
562 87.8% of the logged area, the differences between logged versus unlogged areas are
563 significant Kruskal-Wallis test, $p < 0.05$) (Figure 6). If all forest types are considered,
564 the data suggest the same pattern but the added variation from forest-type effects
565 makes the difference statistically nonsignificant (Figure S-13).
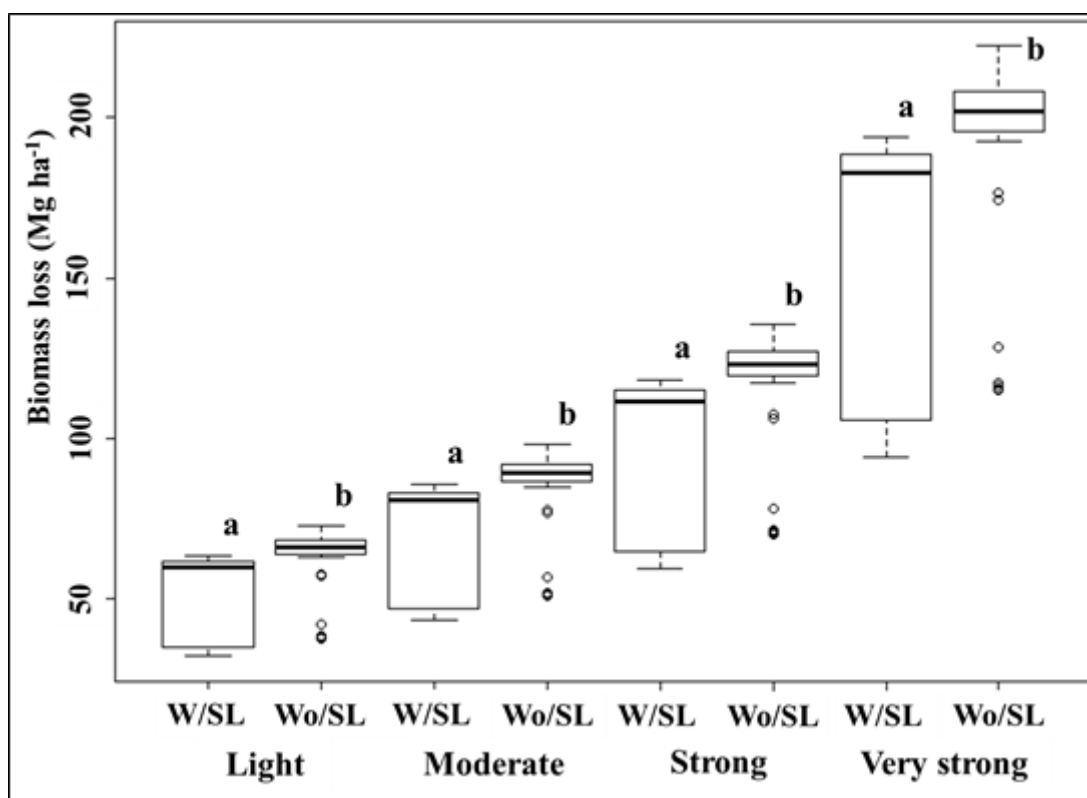
Figure 6. Biomass loss (Mg ha^{-1}) by fire severity class considering areas without SL (Wo/SL) and areas with SL (W/SL) in the study area.

3.6 Calculation of the weights-of-evidence coefficients

Of the 12 variables used to calculate the coefficients of the WEs, six showed a strong correlation between them (r ≥ 0.5). The highest correlation was between cumulative deforestation in the study area and secondary roads, with r = 0.86, and the second-highest value was between SL areas with secondary roads, with r = 0.78 (Table S10). Theoretically, this means that these variables are overlapping in the model and would explain, basically, the same things. When two variables are correlated, it is recommended that one of them be removed from the prediction model, with the variable that remains being the one that is more consistent with the conceptual or theoretical model of the phenomenon to be modeled or predicted (Soares-Filho et al., 2008).

The SL variable (a continuous variable) had the highest value for the weights-of-evidence coefficient (W = +1.15 to 0.99) between 0 to 480 m away from the fires, and this coefficient decreased to a value close to zero at ~2000 m. Similar behavior was also observed for the variables "secondary roads" (W = + 0.68 to 0.83) and "deforestation" (W = + 0.44 to 1.06) in the first 480 m from the areas affected by fires (Figure 7). These distances were expressed as intervals of 120 m in the Dinamica-EGO software and are compatible with the 30-m pixel size of the Landsat 8 image and of the weights-of-evidence maps of the variables used in the study. The response or dependent variable "fire" had the highest weights-of-evidence coefficients. These values indicate a high probability of transition from forest pixels (value=2) located close to the edges of the forest (value=1) to pixels representing burned areas (value=3)

593 on the simulated or modeled map. Note that most of the variables strongly repel the
594 transition of pixels located from ~2500 to 5000 m, with the weights-of-evidence
595 coefficients having values less than zero.
596
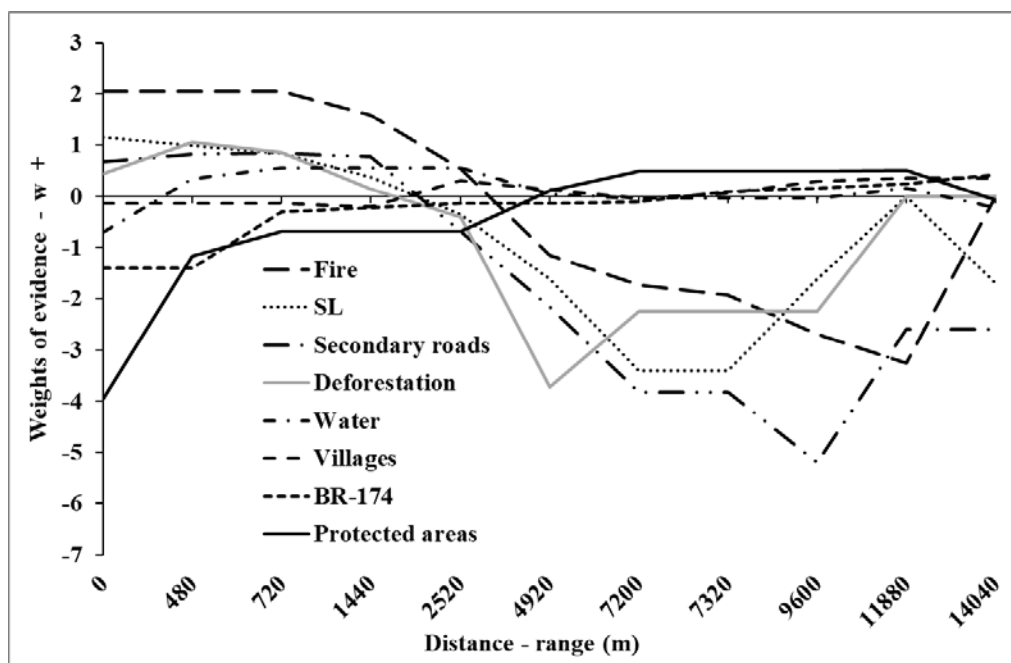
597
598 **Figure 7**. Coefficient of the weights-of-evidence (W $^+$ or W $^-$) for seven variables that explain
599 the occurrence of forest fires (dependent variable) in the study area. The distance is subdivided
600 into multiple intervals of 120 m.

601
602   The behavior of the weights-of-evidence coefficients of SL (and of other variables
603 correlated with SL) shown in Figure 8 can be explained by the heavy fragmentation of
604 the forest in the study area. For example, on both sides of Highway BR-174 there are
605 secondary roads and cumulative deforestation adjacent to these roads (both inside and
606 outside of settlement projects). The roads fragment the forest at regular intervals of 2
607 to 4 km, depending on the degree of deforestation at each site. The sizes of the forest
608 fragments limited the weights-of-evidence (W$^+$) of the main variables that explain the
609 behavior of fire in the study area at distances between 1000 and 2000 m from the edge
610 of the fire scars in the forest (Figure 7).
611   Corroborating these results, the areas affected by forest fires and SL gradually
612 decreased in successive 120-m intervals from the edge of the forest up to a distance of
613 1200 m. The first interval (0 to 120 m) had the largest area affected by fire (114.9 km^2;
614 20.1%) and also had the largest area affected by SL (113.8 km^2; 24.3%). Considering
615 the entire range of 1200 m from the edge of the forest, the area burned totaled 571.7
616 km^2 (83.9% of the 682.2 km^2), SL areas totaled 468.8 km^2 (72.7% of the 644.8 km^2)
617 and the SL areas in areas affected by fire totaled 161.2 km^2, or 89.4% of the 180.4 km^2
618 total (irrespective of distance: Table S15) burned in the SL areas (Figure 8A; Table
619 S15). The ratio of the area affected by SL to the area affected by fire (SL / Fire)
620 showed a continuous growth beginning with the second distance interval (121-240 m
621 from the forest edge) up to a distance of 1200 m (Figure 8B). The SL area affected by
622 fire as a percentage of the SL area as a whole (SL x Fire / SL) had behavior opposite to
623 that of SL / Fire; that is, the areas of occurrence decreased with increasing distance

624 from the edge of the forest. In turn, the area of SL affected by fire as a percentage of
625 the area burned as a whole (SL x Fire / Fire) showed a more stable behavior when
626 compared to the other variables, with 20.6% in the first interval, increasing to 26.5%
627 in the second interval, and stabilizing at 31.1% (on average) from the third to the last
628 interval (360 to 1200 m).
629   These results indicate a strong influence of SL on the spread of the fire in the
630 study area, especially as exemplified by SL / Fire and SL x Fire / Fire (Figure 8B).
631 Although this analysis includes only the variable SL, all other variables were also
632 exposed to the same environmental context in the study area. The values of the
633 weights-of-evidence calculated for each distance range of the variables contained in the
634 models ensure the statistical independence of the results (Bonham-Carter, 1994).
635
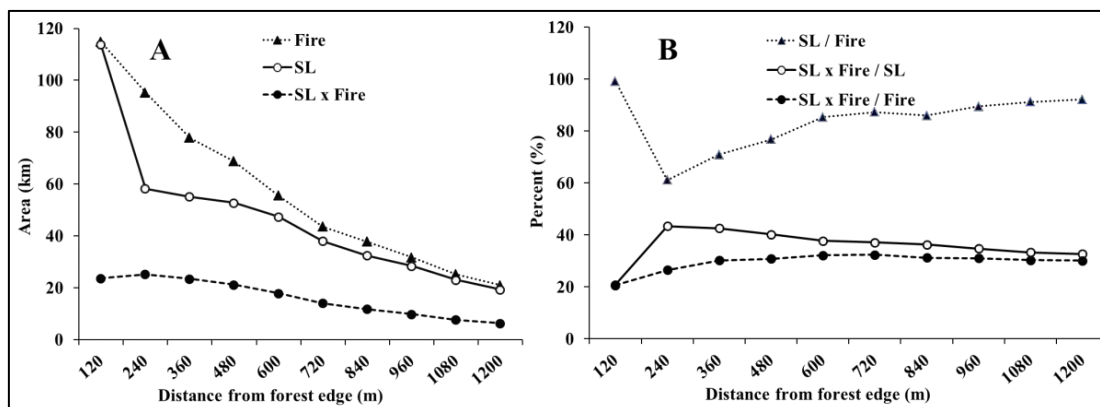
636
637 **Figure 8**. Fire and SL behavior as functions of distance from the forest edge (in 120-m
638 intervals). (**A**) Areas (km^2). (**B**) Interaction between fire and SL (%). Fire = Area affected by
639 fire; SL = Area of SL; SL x Fire = Area of SL affected by fir; SL / Fire = Ratio of the
640 area affected by SL to the area affected by fire; SL x Fire / SL = The SL area affected
641 by fire as a percentage of the SL area as a whole; SL x Fire / Fire = Area of SL
642 affected by fire as a percentage of the area burned as a whole.
643
644 **3.7 Model-validation results**

645   The models were validated in windows that ranged in size from one pixel (30 m)
646 to seven pixels (210 m). The average similarity observed in these windows,
647 considering all models, was 63.3%. The map using all variables in the model obtained
648 the greatest similarity between the modeled maps and the fire observed in 2016,
649 reaching 50% similarity in a ~70-m window. On the other hand, the worst
650 performance was by the map from the model that used only the variables that were not
651 correlated, reaching 50% similarity in a ~112-m window. The other three models had
652 approximately the same performance, with results between the two extremes and
653 reaching 50% similarity in a window of ~80-m (Figure S10).

654   .
655 **3.8 Vulnerability of the forest to understory fires by probability range**

656   Considering ranges of vulnerability to the occurrence of forest fires in the
657 probability map, areas vulnerable to fire increased by 266.2% in the range with the
658 highest vulnerability when SL and SL class year were present, as compared to the
659 reference model (Figure S11). Likewise, when the probability map was modeled with

660 the presence of secondary roads, the area of greatest vulnerability to fire increased by
661 360.4% compared to the reference model (Figure 9; Table S16).
662
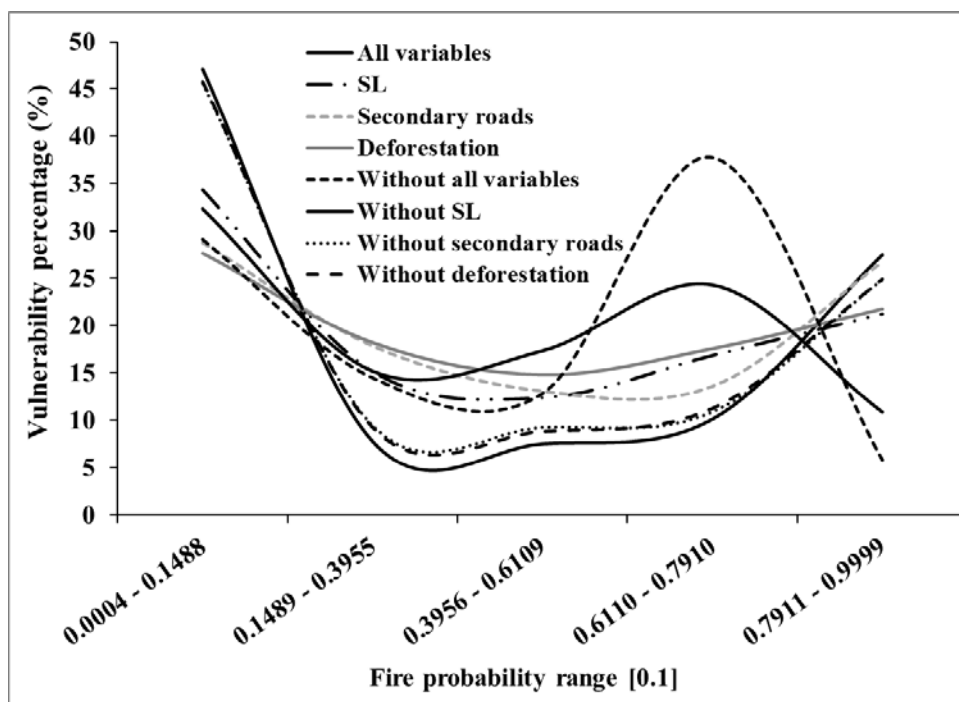
663
664 **Figure 9**. Percentage of vulnerability of the forest as a function of the ranges of probability
665 (0.1) of fire occurrence in the study area.
666
667   All of the vulnerability maps had the class with the lowest probability of fire
668 (0.0004 to 0.1488) as the most representative area in the modeling. This can be
669 explained simply by the fact that these areas are relatively far from the sources of
670 ignition by human action and, therefore, would be naturally protected. This can be
671 clearly seen in continuous blocks of forest on both sides of Highway BR-174 in the
672 map calculated with the entire set of variables (areas south of Vila Colina in the south-
673 central part of the map) (Figure 10A). To a lesser extent it can also be seen in Figure
674 10C. On the other hand, the map considered as a reference, which represented fires
675 calculated by the model composed of three explanatory variables not correlated with
676 the SL (altitude, slope, and vegetation) (Figure 10B), showed these blocks of forest as
677 vulnerable to fire. This effect can be explained by the absence of protected areas in the
678 model's data set. Because the protected areas were correlated with SL, this effect was
679 less evident in the calculated map containing SL in the data set. The maps of
680 vulnerability to fires calculated with the variables "secondary roads" and
681 "deforestation" are shown in Figure S12.
682
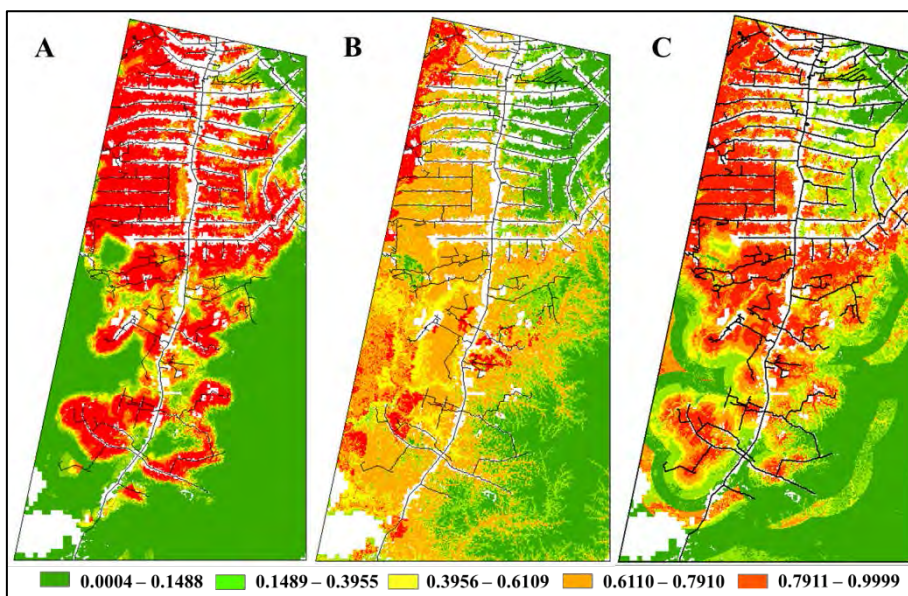
Figure 10. Maps of vulnerability of the forest to understory fire. In (A) forest vulnerability map calculated with the entire set of variables (n = 12). In (B) vulnerability map calculated from a set of three variables (altitude, vegetation and slope) that are not correlated with SL (reference model). In (C) forest vulnerability map calculated from the variables not correlated with SL and plus the SL and SL class year variables. The legend below the figure shows the ranges of probability [0.1] of the forest being affected by fires.

The exposure of forest biomass to fires in the study area was 457.2% higher when considering the variable "cumulative deforestation" compared to the reference model (Figure 10B), while SL and SL class year exposed 407.0 % more forest biomass when compared to the reference model. This percentage (400.7 %) can be considered to represent the effect of SL on the spread of fire in the study area. The variable "secondary roads" exposed 591.2% more biomass to fire than the reference model (Figure 11). Likewise, SL and SL class year exposed 266.2% more forest area to the range with the highest risk of vulnerability compared to the reference map, while deforestation exposed 9.0% more area than SL. Back roads exposed 360.4% more forest area than the reference map (Figure S11).
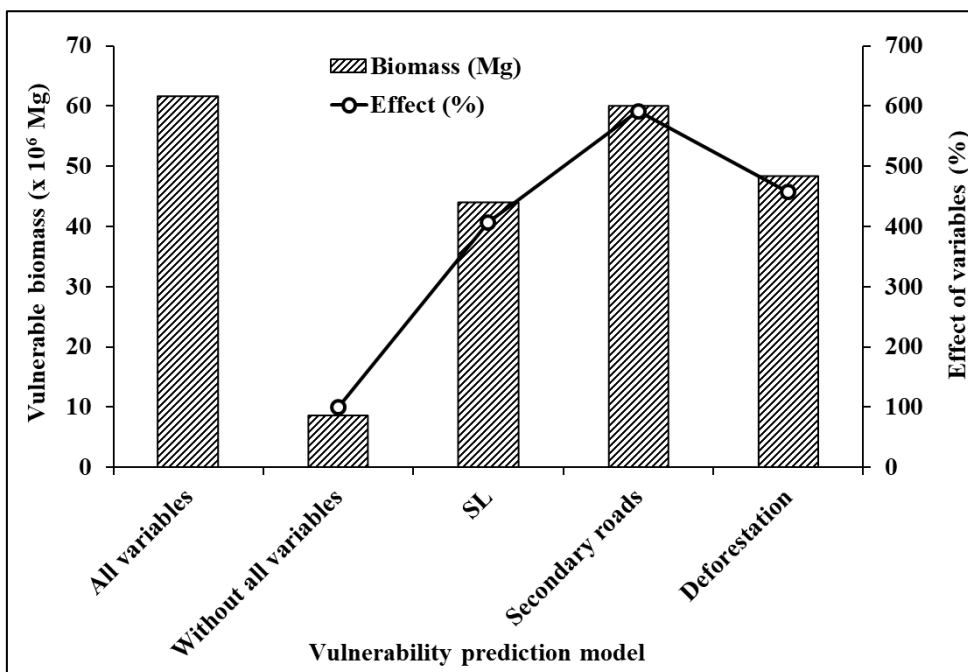
Figure 11. Biomass vulnerable to understory forest fires in the study area.

3.9 Effect of logging on biomass losses due to fire

The biomass losses in burned areas are summarized in Table 6, indicating a total loss of 5.22×10^6 Mg of biomass stock due to fire. In the burned areas the percentage of biomass lost is 23.2% in areas that had been selectively logged, and 21.6 % in areas without selective logging.

The effects of selective logging on losses to fire are calculated in Table 7. The effect of logging in increasing the area burned resulted in 1.22×10^6 Mg of biomass loss due to fire (Column G), while the effect of selective logging in increasing the severity of fire and resulting per-hectare biomass loss in the area that would have burned anyway even without logging represents 1.25×10^6 Mg of biomass loss (Column M). As compared to the biomass loss from the logging itself (including collateral damage) of 1.69×10^6 Mg of biomass, the effect of logging on increasing the area burned increases impact by 72.5% (Column AB), and the increased fire severity increases the total fire impact to 146.5% (Column AD), that is, more than doubling the impact of the logging itself.

723
724

Table 6. Summary of biomass losses in burned areas

	Original forest (unlogged and unburned)			SL loss			Affected by fire		Loss to fire		
	Area	Biomass stock	Biomass per hectare	Percent of original biomass	Biomass stock	Biomass per hectare	Biomass stock	Biomass per hectare	Biomass stock	Biomass per hectare	Percent affected biomass
	(km^2)	$(10^6\ Mg)$	$(Mg\ ha^{-1})$	(%)	$(10^6\ Mg)$	$(Mg\ ha^{-1})$	$(10^6\ Mg)$	$(Mg\ ha^{-1})$	$(10^6\ Mg)$	$(Mg\ ha^{-1})$	(%)
Burned areas with SL in ombrophilous forest	152.3	6.63	435.1	8.2	0.54	35.7	6.08	399.4	1.48	97.2	24.3
Burned areas without SL in ombrophilous forest	380.3	16.60	436.5	0	0	0	16.60	436.5	3.58	94.2	21.6
Total in ombrophilous forest	532.6	23.23	436.1	2.3	0.54	35.7	22.68	425.9	5.06	95.1	22.3
Burned areas with SL in *campinarana*	28.3	0.71	250.7	8.2	0.06	20.6	0.65	230.1	0.16	56.0	24.3
Burned areas without SL in *campinarana*	111.7	2.87	256.8	0	0	0	2.87	256.8	0.63	56.1	21.8
Total in *campinarana*	140.0	3.58	255.6	1.6	0.06	20.6	3.52	251.4	0.78	56.1	22.3
Burned areas with SL in ecotone forest	1.2	0.04	333.3	8.2	0.0033	27.3	0.04	306.0	0.07	86.3	28.2
Burned areas without SL in ecotone forest	8.1	0.30	370.4	0	0	0	0.26	321.0	0.06	69.8	21.6
Total in ecotone forest	9.3	0.30	323.3	0	0	0	0.30	319.8	0.13	70.1	22.1
Burned areas with SL in all forest types	180.6	7.34	406.2	8.2	0.60	33.3	6.73	372.9	1.64	90.8	24.3
Burned areas without SL in all forest types	501.3	19.77	394.4	0	0	0	19.47	388.4	4.21	84.0	21.6
Total in all forest types	681.9	27.10	397.5	2.2	0.60	33.3	26.20	384.3	5.85	85.8	22.3

725

Table 7. Effect of logging on area and biomass burned

Forest type	A	B	C	D	E	F	G	H	I
	Total area burned (km^2)	Area burned w/SL (km^2)	Area burned that would have remained unburned w/oSL (km^2)	Average post-logging biomass in area w/SL (Mg ha^{-1})	Fraction killed by fire W/SL	Average biomass killed by fire in burned area that would have remained unburned w/o SL (Mg ha^{-1})	Total biomass killed by fire in burned area that would have remained unburned (10^6 Mg)	Fraction killed by fire Wo/SL	Area that Would have burned if there had been no SL in areas that had SL (km^2)
Source	Table 6	Table 6	B - I	Table 4	Table 5	D × E	C × 100 × F/10^6	Table 6	B - C
Ombrophilous	532.7	152.3		399.6	0.232	92.6		0.216	
Campinarana	140.0	28.3		230.3	0.232	53.4		0.218	
Ecotone	9.3	0		'--	'--	'--		0.194	
All types	681.9	180.6	138.4	384.2	0.232	89.1	1.22	0.216	43.4

726

	J	K	L	M	N	O	P	Q	R
	Additional fraction burned W/SL as compared to Wo/SL	Average additional biomass killed by fire in area W/SL that would have Burned w/o SL (Mg ha^{-1})	Total additional biomass killed by fire in area W/SL that would have burned w/o SL (10^6 Mg)	Total additional biomass killed by fire due to SL (10^6 Mg)	Fraction of original biomass removed or killed by SL	Average biomass Wo/SL (Mg ha^{-1})	Average biomass removed or killed by SL (Mg ha^{-1})	Total biomass removed or killed by SL in study Area w/SL (10^6 Mg)	Percent increase of impact of SL due to additional area burned (%)
Source	E - H	D × S	((B-D)×100-T) /10^6	G + U	Section 2.3.2	Table 6	W × X	T×100×Y /10^6	V/Z×100
Ombrophilous	0.016	6.4			0.082	435.0	35.7	0.54	
Campinarana	0.014	3.1			0.082	250.8	20.6	0.06	
Ecotone	--	--			--	360.3	--	0	
All types	0.016	6.0	0.03	1.25	0.082	395.0	32.3	1.69	74.1

727

	S	T	U	V	W	X
	Total area present (km²)	Total area logged (km²)	Total area not logged (km²)	Total area burned w/SL (km²)	Total area burned wo/SL (km²)	Total area burned (km²)
Source	Table S-13	Section 4.2.2	S - T	Table 6	Table 6	V + W
Ombrophilous	5,720.8			152.3	380.3	532.7
Campinarana	727.9			28.3	111.7	140.0
Ecotone	63.7			0.0	9.3	9.3
All types	6,512.4	520.5	5,991.9	180.6	501.3	681.9

	Y	Z	AA	AB	AC	AD
	Percent burned of area logged (%)	Percent burned of area not logged (%)	Area that would have burned in logged area if unlogged (km²)	Loss from fire due to logging effect on burned area as % of loss from logging (%)	Total biomass loss from fire due to logging (10⁶ Mg)	Biomass loss from fire due to logging as % of loss from logging (%)
Source	V/T ×100	W/U ×100	Z/100×AJ	G/Q×100	G + M	AC/Q×100
All types	34.7	8.4	43.5	72.5	2.47	146.5

729
730
4. Discussion
4.1 Role of selective logging in increasing fire severity

In our study, the use of severity classes based on NDVI offered excellent insights into the severity of SL practiced in the studied area. Our approach can be considered to be a methodological advance because it can be easily used in calculating GHG emissions to the atmosphere using land-use models, reducing uncertainties, for example at the scale of Landsat pixels. Although it is a simplification for calculations of biomass loss, the use of constant values in our study (Table 2) can be justified by the difficulty (logistics and trained professionals) of obtaining the true parameters for the forest affected by the fires. This explains, in part, why the Brazilian inventories of greenhouse-gas emissions do not yet consider emissions from forest degradation by understory forest fires and selective logging (e.g., Brazil, MCTI, 2020).

The highest occurrences of burned areas and SL in the first distance intervals from the edge are characteristic of the intense fragmentation of the forest caused by human occupation in the study area. This fragmentation increases the contact between the sources of fire ignition (burning of forest biomass from deforestation and in the management of pastures and agricultural fields) and the edge of the forest (Alencar et al., 2006, 2015; Aragão and Shimabukuro, 2010).

Estimates of the biomass in areas affected by logging must be adjusted for the amounts of biomass removed by the logging. Logging slash and additional trees killed in the logging operations will remain in the forest as dead biomass (necromass) and the carbon in these components will eventually be emitted to the atmosphere either through burning or decay. An idea of the harvest intensity of the selective logging in the area can be derived from the officially reported volumes processed by sawmills in the municipality: a total of 455,347 m^3 over the 2007-2015 period (Brazil, IBGE, 2021). Although the part of our study area in Rorainópolis (Table S1) represents only 19.1% of the area of the municipality (33,579.7 km^2), it represents virtually all of the accessible area of forest outside of protected areas. The concentration of logging pressure in a relatively small space in the municipality may have induced the loggers to exploit these forest resources at high intensity, exposing the forest to greater fire hazard. On the other hand, the concentration of logging in a small area protected the currently inaccessible areas from increased fire risk.

4.2 Logging intensities in SL

Logging in the southern portion of the state is practiced in a manner similar to that practiced in other parts of the Brazilian Amazon (Nepstad et al., 1999). Like other areas in the Amazon, logging in our study area is characterized by exploitation of only a few commercial species, a low yield of sawn wood, deficiency in the application of forest management and widespread illegality in removal of wood from the forest (G1, 2018b; Gimenez et al., 2015; Lentini et al., 2005; Monteiro et al., 2010; Pereira et al., 2010).

The estimate of logging intensity that is needed in order to calculate the biomass present in the logged areas at the time of the 2015-2016 fires requires deduction based on the volume of logs removed and the area we mapped as affected by SL (see Supplementary Material, Section 1.7). Officially, from 2010 to 2015, 350,147.0 m^3 of

776 logs were harvested in the municipality of Rorainópolis (Brazil, IBGE, 2021). If we
777 consider that all of this volume of wood was obtained exclusively from our study area,
778 where the areas authorized for deforestation totaled 124.8 km^2 in the period from 2010
779 to 2015, the average volume removed would be 28.1 m^3 ha^{-1}. Although this value is
780 44.8% higher than the value used in our calculations, in terms of volume (19.4 m^3 ha^{-1}
781), to deduct biomass removed by SL (35.67 Mg ha^{-1}; Supplementary material: Section
782 1.8) in areas that were burned and had signs of SL, the generated volume reaches
783 1,009,770 m^3 in 520.5 km^2 of SL polygons (19.4 × 520.5 × 100) mapped in our study
784 area from 2010 to 2015 (Table S8). This value indicates that there may have been a
785 logging 2.9 times (188.4%) greater than the value officially reported by the loggers
786 (Brazil, IBGE, 2021).
787
788   Authorized forest-management projects provide another basis for comparison.
789 Although FEMARH did not provide data on authorized forest-management plans for
790 our study area before 2016, if we assume that in the period from 2010 to 2015 the
791 same area was authorized annually for management as occurred between 2016 and
792 2019 (1566.6 ha year^{-1}) (i.e., before the substantial increase in authorization in 2020),
793 and we apply the average authorized harvest of 24 m^3 ha^{-1}, this implies an annual
794 authorized harvest of 37,597.2 m^3 (Table S4). The total volume from deforestation
795 authorizations in the 2010-2015 period (611,674.9 m^3; Table S3), plus the assumed
796 forest-management authorizations (225,583.2 m^3) total 837,758.1 m^3, or 2.4 times the
797 350,147 m^3 officially reported as harvested in the municipality in the same period
798 (Brazil, IBGE, 2021). This probably means that the officially reported volume is
799 greatly understated.
800   Considering the 520.5 km^2 of SL area mapped between 2010 and 2015 (Table S8)
801 and, using the same average harvest of 24 m^3 ha^{-1}, the total exploited volume would be
802 1,249,200.0 m^3, or ~3.6 times higher than that reported by Brazil, IBGE (2021) for the
803 same time interval. Another important factor to be considered is that only 26.2%
804 (3114.1 ha) of the area authorized for "alternative land use" between 2010 and 2015
805 (12,480.9 ha) was effectively deforested by 2020. These facts hide a serious problem
806 for the timber sector in southern Roraima and explains, in part, why many lumber
807 companies were closed and stopped working after IBAMA inspection operations in
808 Rorainópolis (G1, 2018a) and in the port of Manaus, Amazonas (G1, 2018b). In
809 addition, it supports the supposition that permits for SL in areas released for
810 "alternative land use" (deforestation) are used to launder wood.
811
812 **4.3 Wood laundering as a factor in selective logging and consequent fire**

813   While the 2015-2016 El Niño provided ideal climatic conditions for fires (Aragão
814 et al., 2018; Burton et al., 2020; Fonseca et al., 2017; Ray et al., 2005), much of the
815 "blame" for the fires and the damage they caused can be attributed to the roles of SL in
816 increasing the probability of areas being burned and in increasing the damage when
817 burning occurs. The large area of selective logging in our study area appears to be
818 mainly the result of permits from authorized deforestation being used to provide cover
819 for transporting the logs to sawmills (i.e., "laundering" wood) and a lesser amount
820 from authorized forest-management projects.
821   In our study area logging is done based on the approval of licenses for clearing
822 forest for agriculture and pasture. In these projects FEMARH authorizes the sale of a

823   restricted volume of wood, which generally varies between 20 and 100 m³ per ha of
824   authorized clearing (e.g., Barni et al., 2020). These authorizations are often used to
825   "launder" wood from illegal logging in nearby forests, including wood from outside of
826   the properties where the clearcutting was licensed (Condé et al., 2019). In these
827   clearcutting projects, the wood is harvested before the forest is cleared, and one to two
828   years or more elapse before the remaining trees are cut when the area is deforested for
829   pasture (this is recurrent throughout the southern portion of the state). In this case, the
830   forest contains large clearings resulting from the opening of roads and log-storage
831   yards, with the remaining trees left standing until the end of the logging operation
832   before being cut. The burning of areas that are deforested in clearcutting projects serve
833   as sources of ignition for the spread of fire to the adjacent forest. Logging disturbance
834   can be more serious than the deforestation itself as a force for spreading fire. Under
835   extreme climatic conditions such as the 2015/2016 El Niño event (Burton et al., 2020;
836   Fonseca et al., 2017), logged areas become highly vulnerable to fires (Andrade et al.,
837   2020; Cochrane et al., 1999; de Faria et al., 2017; Morton et al., 2011; Ziccardi et al.,
838   2019). The logged areas serve as "springboards" for fire to gain momentum and spread
839   to adjacent areas, including those without evidence of SL.
840   This effect of recent logging was shown by the correlation analysis between the
841   incidence of fire and the difference between the NDVI values observed in SL areas
842   carried out in years immediately before the fires and the NDVI values observed in the
843   same places in 2016 (Figure S9). The increasing correlation between these values over
844   time is consistent with the more recently logged areas having greater fire severity
845   (Figure 5B). This corroborates the studies by Souza Jr. et al. (2005a, 2013), who
846   analyzed forest degradation by SL and fire using multitemporal images.

847   **4.4 Vulnerability of the forest to understory fires**

848   The variables that contributed the most to the vulnerability of the forest were, in
849   decreasing order, the distance from secondary roads, the distance from previous or
850   cumulative deforestation and the distance from selective logging. The effects of major
851   and secondary roads on the occurrence of deforestation and forest fires in the Amazon
852   are well known (Barni et al., 2015b; Fonseca et al., 2017, 2019; Silvestrini et al., 2011;
853   Soares-Filho et al., 2006). However, with regard to modeling the risk of forest fire
854   using SL as an explanatory variable in the model, our results are unprecedented and
855   demonstrate the importance of regulating this activity for combating and controlling
856   forest fires in Brazilian Amazonia.
857   Modeling the probability of the occurrence of fires in the study area using the
858   weights-of-evidence method allowed us to produce a vulnerability map of the forest
859   (map with all variables) with very high spatial resolution (compatible with the Landsat
860   8 pixel size of 30 m). Providing information for use in risk maps for the occurrence of
861   catastrophic events, such as floods, hurricanes and forest fires, is valuable for planning
862   and for preventing and mitigating the potential impacts these calamities cause to the
863   economic, social and environmental sectors. Increasing the accuracy of models can
864   make them more effective as a basis for public policies to reduce these risks (Ferrier et
865   al., 2016; Fonseca et al., 2017, 2019; Marcelino, 2008). The map of forest
866   vulnerability to fire modeled in this study can serve as a tool for planning preventive
867   measures for combating fires and for mitigating the effects of fire in Roraima (Barbosa
868   et al., 2003). The increased vulnerability of selectively logged forest to fire implies

869 that the simple assumption that authorized forest management projects in Amazonia
870 are sustainable is unwarranted. One cannot simply assume that if government
871 regulations on the intensity of logging and other factors in management systems are
872 followed then the system will automatically be sustainable. Unfortunately, fire was not
873 considered in the forest-recovery studies underlying official regulations. Virtually all
874 plans for forest management in Amazonia assume that the managed areas will never
875 burn (see Fearnside, 2003). The falseness of this assumption is central to discussions
876 of the appropriate role of forest management in Amazonian development.
877   The roles of selective logging in facilitating forest fires and increasing their
878 damage mean that SL can have harmful and unpredictable consequences for the
879 structure of the forest (Rappaport et al., 2018). Fires also affect the forest's health,
880 with repercussions for the survival of arboreal individuals in the years following the
881 fires (Andrade et al., 2020; Avila et al., 2018; Trumbore et al., 2015; Watson et al.,
882 2018; Ziccardi et al., 2019). The increase in fire severity provoked by logging implies
883 direct impacts on greenhouse-gas emissions and global climate (Aragão et al., 2007,
884 Assis et al., 2020, 2018; de Faria et al., 2017; Rappaport et al., 2018; Stark et al., 2020;
885 Trumbore et al., 2015). Fires like these are known to initiate a positive-feedback
886 process, where the fire leaves dead wood in the forest that serves as fuel for the next
887 fire at the time of another extreme drought event, making this and subsequent fires
888 more intense, and this can completely destroy an area of forest after three or four fires
889 (Berenguer et al., 2014; Cochrane et al., 1999; Nepstad et al., 1999). The effect of fire
890 in more than doubling the impact of the logging itself, increasing the impact by
891 146.5%, affects the calculus for forest management. This level of impact is the result
892 of a single fire, and this is only the beginning of the positive feedback process of
893 degradation in a downward spiral of biomass stocks. The large impact of selective
894 logging through the effect on fire should both serve as a warning to policy makers
895 promoting forest management and add urgency to repressing the widespread illegal
896 logging in Amazonia.
897

898 **5. Conclusions**

899   The methods developed here to estimate the effects of selective logging based on
900 fire-severity classes and the modeling of fire spread based on weights-of-evidence can
901 be used as a tool for creating public policies regarding logging and fire. The results
902 these policies need to be more cautious in promoting forest management and more
903 rigorous in controlling illegal logging, as well as increasing efforts to prevent fires.
904   The selective logging practiced in the southern portion of Roraima contributed
905 significantly to the increase in damage to forest biomass and consequent emission of
906 carbon to the atmosphere, in addition to facilitating the spreading of forest fires and
907 increasing their intensity. If a hectare of forest is burned, the fire intensity is 85.9%
908 more likely to be in the "very strong" category if it had been previously logged. Fire
909 increased the impact of logging on biomass reduction by 146.5% as compared to the
910 impact of the logging itself, thus more than doubling the impact of logging with just
911 one fire. These results cast doubt on the assumption that approved forest-management
912 projects are sustainable on the long term. In addition, the connection of logging
913 disturbance and resulting forest fires to authorized wood sales from areas licensed for

914 clearcutting indicates the need for Roraima's environmental agency (FEMARH) to
915 revise its policies on the use of wood from forest-clearing projects.
916

917 **6. Acknowledgments**

927

928 **7. References**

929 Alencar, A., Nepstad, D., Diaz, M.D.V., 2006. Forest understory fire in the Brazilian
930   Amazon in ENSO and non-ENSO years: Area burned and committed carbon
931   emissions. Earth Interactions, 10, art. 6. https://doi.org/10.1175/EI150.1.

932 Alencar, A.A., Brando, P.M., Asner, G.P., Putz, F.E., 2015. Landscape fragmentation,
933   severe drought and the new Amazon forest fire regime. Ecological Applications,
934   25(6), 1493–1505. https://doi.org/10.1890/14-1528.1.

935 Alvares, C.A., Stape, J.L., Sentelhas, P.C., Gonçalves, J.L.M., Sparovek, G., 2014.
936   Köppen's climate classification map for Brazil. Meteorologische Zeitschrift,
937   22(6), 711–728. https://doi.org/10.1127/0941-2948/2013/0507

938 Andrade, D.F.C., Ruschel, A.R., Schwartz, G., de Carvalho, J.O.P., Humphries, S.,
939   Gama, J.R.V., 2020. Forest resilience to fire in eastern Amazon depends on the
940   intensity of prefire disturbance. Forest Ecology and Management, 472, art.
941   118258. https://doi.org/10.1016/j.foreco.2020.118258.

942 Aragão, L.E.O.C., Malhi, Y., Roman-Cuesta, R.M., Saatchi, S., Anderson, L.O.,
943   Shimabukuro, Y.E., 2007. Spatial patterns and fire response of recent Amazonian
944   droughts. Geophysical Research Letters, 34(7), art. L07701.
945   https://doi.org/10.1029/2006GL028946.

946 Aragão, L.E.O.C, Shimabukuro, Y.E. 2010. The incidence of fire in Amazonian
947   forests with implications for REDD. Science, 328, 1275-1278.
948   https://doi.org/10.1126/science.1186925.

949 Aragão, L.E.O.C, Anderson, L.O., Fonseca, M.G.. Rosan, T.M., Vedovato, L.B.,
950   Wagner, F.H., Silva, C.V.J., Silva Junior, C.H.L., Arai, E., Aguiar, A.P. et al.,
951   2018. 21st Century drought-related fires counteract the decline of Amazon
952   deforestation carbon emissions. Nature Communications, 9, art. 536.
953   https://doi.org/10.1038/s41467-017-02771-y.

954 Assis, T.O., Aguiar, A.P.D., von Randow, C., Gomes, D.M.P., Kury, J.N., Ometto,
955   J.P.H.B., Nobre, C.A., 2020. CO_2 emissions from forest degradation in Brazilian

956   Amazonia. Environmental Research Letters, 15(10), art. 104035.
957   https://doi.org/10.1088/1748-9326/ab9cfc.

958 Avila, A.L., Schwartz, G., Ruschel, A.R., Silva, J.N.M., de Carvalho, J.O.P., Mazzei,
959   L., Soares, M.H.M., Bauhus, J., 2017. Recruitment, growth and recovery of
960   commercial tree species over 30 years following logging and thinning in a tropical
961   rain forest. Forest Ecology and Management, 385, 225–235.
962   https://doi.org/10.1016/j.foreco.2016.11.039.

963 Baccini, A., Goetz, S.J., Walker, W.S., Laporte, N.T., Sun, M., Sulla-Menashe, D.,
964   Hackler, J., Beck, P.S.A., Dubayah, R., Friedl, M.A., Samanta S., Houghton, R.A.,
965   2012. Estimated carbon dioxide emissions from tropical deforestation improved
966   by carbon-density maps. Nature Climate Change, 2, 182–185.
967   https://doi.org/10.1038/NCLIMATE1354.

968 Barbosa, R.I., Fearnside, P.M., 1999. Incêndios na Amazônia: Estimativa da emissão
969   de gases de efeito estufa pela queima de diferentes ecossistemas de Roraima na
970   passagem do evento El-Niño (1997/1998). Acta Amazonica, 29(4), 513-534.
971   https://doi.org/10.1590/1809-43921999294534.

972 Barbosa, R.I., Xaud, M.R., Silva, G.N.F., Cattâneo, A.C., 2003. Forest Fires in
973   Roraima, Brazilian Amazonia. International Forest Fire News (IFFN), No. 28, 51-
974   56. https://gfmc.online/wp-content/uploads/Brazil-2-1.pdf

975 Barlow, J., Peres, C., Lagan, B., Haugaasen, T., 2003. Large tree mortality and the
976   decline of forest biomass following Amazonian wildfires. Ecology Letters, 6, 6–8.
977   https://doi.org/10.1046/j.1461-0248.2003.00394.x.

978 Barni, P.E., Silva, E.B.R., 2017. Extração seletiva de madeira em Rorainópolis: A
979   floresta em perigo. In: Anais da Semana Nacional de Ciência e Tecnologia no
980   estado de Roraima: Ciência alimentando Brasil. Universidade Estadual de
981   Roraima (UERR), Boa Vista, RR. art. 36103. https://bityl.co/5JbX. Accessed on:
982   23 January 2021.

983 Barni, P.E., Silva, E.B.R., Silva, F.C.F., 2017. Incêndios florestais de sub-bosque na
984   zona de florestas úmidas do sul de Roraima: Área atingida e biomassa morta. In:
985   Anais do Simpósio Brasileiro de Sensoriamento Remoto 2017. Campinas, SP,
986   Brazil: Galoá, pp. 6280-6287. Available at: https://bityl.co/5JeV. Accessed on: 21
987   November 2020.

988 Barni, P.E., Pereira, V.B., Manzi, A.O., Barbosa, R.I., 2015a. Deforestation and forest
989   fires in Roraima and their relationship with phytoclimatic regions in the northern
990   Brazilian Amazon. Environmental Management, 55, 1124–1138.
991   https://doi.org/10.1007/s00267-015-0447-7.

992 Barni, P.E., Fearnside, P.M., Graça, P.M.L.A., 2015b. Simulating deforestation and
993   carbon loss in Amazonia: Impacts in Brazil's Roraima state from reconstructing
994   Highway BR-319 (Manaus-Porto Velho). Environmental Management, 55(2),
995   259-278. https://doi.org/10.1007/s00267-014-0408-6.

996 Barni, P.E., Manzi, A.O., Condé, T.M., Barbosa, R.I., Fearnside, P.M., 2016. Spatial
997   distribution of forest biomass in Brazil's state of Roraima, northern Amazonia.

998   Forest Ecology and Management, 377, 170–181.
999   https://doi.org/10.1016/j.foreco.2016.07.010.

1000 Barni, P.E., Barbosa, R.I., Manzi, A.O., Fearnside, P.M., 2020. Simulated
1001   deforestation versus satellite data in Roraima, northern Amazonia, Brazil.
1002   Sustentabilidade em Debate, 11(2), 81-94.
1003   https://doi.org/10.18472/SustDeb.v11n2.2020.27493.

1004 Bastarrika, A., Chuvieco, E., Martín, M.P. 2011. Automatic burned land mapping
1005   from MODIS time series images: assessment in Mediterranean ecosystems. IEEE
1006   Transactions on Geoscience and Remote Sensing, 49(9), 3401-3413.
1007   https://doi.org/10.1109/TGRS.2011.2128327

1008 Berenguer, E., Ferreira, J., Gardner, T.A., Aragão, L.E.O.C., de Camargo, P.B., Cerri,
1009   C.E., Durigan, M., de Oliveira Jr., R.C., Vieira, I.C.G., Barlow, J., 2014. A large-
1010   scale field assessment of carbon stocks in human-modified tropical forests. Global
1011   Change Biology, 20(12), 3713–3726. https://doi.org/10.1111/gcb.12627

1012 Bonham-Carter, G., 1994. Geographic Information Systems for Geoscientists:
1013   Modeling with GIS. New York, USA: Pergamon. 398 pp.

1014 Brancalion, P.H.S., de Almeida, D.R.A., Vidal, E., Molin, P.G., Sontag, V.E., Souza,
1015   S.E.X.F., Schulze, M.D. 2018. Fake legal logging in the Brazilian Amazon.
1016   Science Advances, 4, art. eaat1192. https://doi.org/10.1126/sciadv.aat1192

1017 Brando, P.M., Balch, J.K., Nepstad, D.C., Morton, D.C., Putz, F.E., Coe, M.T.,
1018   Silvério, D., Macedo, M.N., Davidson, E.A., Nóbrega, C.C., Alencar, A., Soares-
1019   Filho, B.S., 2014. Abrupt increases in Amazonian tree mortality due to drought–
1020   fire interactions. Proceedings of the National Academy of Sciences of the USA,
1021   111(17), 6347-6352. https://doi.org/10.1073/pnas.1305499111.

1022 Brando, P.M., Paolucci, L., Ummenhofer, C.C., Ordway, E.M., Hartmann, H., Cattau,
1023   M.E., et al., 2019. Droughts, wildfires, and forest carbon cycling: A pantropical
1024   synthesis. Annual Review of Earth and Planetary Sciences, 47, 555-581.
1025   https://doi.org/10.1146/annurev-earth-082517-010235.

1026 Brazil, IBGE (Instituto Brasileiro de Geografia e Estatística), 2021. Produção da
1027   Extração Vegetal e da Silvicultura: Tabela 289. Available at:
1028   https://sidra.ibge.gov.br/Tabela/289. Accessed on: 19 March 2021.

1029 Brazil, INPE (Instituto Nacional de Pesquisas Espaciais), 2020. Projeto PRODES –
1030   Monitoramento da Floresta Amazônica por Satélite. São José dos Campos, SP,
1031   Brazil: INPE. Available at: https://bityl.co/5JeS. Accessed on: 21 November 2020.

1032 Brazil, MCTI (Ministério da Ciência, Tecnologia e Inovação), 2020. Estimativas
1033   Anuais de Emissões de Gases de Efeito Estufa no Brasil. Quinta edição. 108 pp.,
1034   Available at: https://bityl.co/5JeH. Accessed on: 21 November 2020.

1035 Brazil, PROBio (Projeto da Biodiversidade Brasileira), 2013. Mapas de Cobertura
1036   Vegetal dos Biomas Brasileiros. Available at: https://bityl.co/5JeR. Accessed on:
1037   21 November 2020.

1038 Brazil, RADAMBRASIL, 1973–1983. Levantamento dos Recursos Naturais (Folhas
1039   SA.20 Manaus; SA.21 Santarém; SB.19 Juruá; SB.20 Purus; SC.19 Rio Branco;
1040   SC.20 Porto Velho). Rio de Janeiro, RJ, Brazil: Ministério das Minas e Energia.

1041 Broadbent, E.N., Asner, G.P., Keller, M., Knapp, D.E., Oliveira, P.J.C., Silva, J.N.,
1042   2008. Forest fragmentation and edge effects from deforestation and selective
1043   logging in the Brazilian Amazon. Biological Conservation, 141, 1745-1757.
1044   https://doi.org/10.1016/j.biocon.2008.04.024

1045 Burton, C., Betts, R.A., Jones, C.D., Feldpausch, T.R., Cardoso, M., Anderson, L.O.,
1046   2020. El Niño driven changes in global fire 2015/16. Frontiers in Earth Science, 8,
1047   1-12. https://doi.org/10.3389/feart.2020.00199.

1048 Chuvieco, E., Martín, M.P., Palacios, A. 2002. Assessment of different spectral
1049   indices in the red-near infrared spectral domain of burned land discrimination.
1050   International Journal of Remote Sensing, 23, 5103-5110.
1051   https://doi.org/10.1080/01431160210153129

1052 Cochrane, M.A., Alencar, A., Schulze, M., Souza Jr., C., Nepstad, D.C., Lefebvre, P.,
1053   Davidson, E., 1999. Positive feedbacks in the fire dynamic of closed canopy
1054   tropical forests. Science, 284, 1832–1835.
1055   https://doi.org/10.1126/science.284.5421.1832.

1056 Cohen, J., 1988. Statistical power analysis for the behavioral sciences. Hillsdale, NJ,
1057   USA: Erlbaum. Available at:
1058   http://www.utstat.toronto.edu/~brunner/oldclass/378f16/readings/CohenPower.pdf
1059   . Accessed on: 2 April 2021.

1060 Condé, T.M., Higuchi, N., Lima, A.J.N., 2019. Illegal selective logging and forest
1061   fires in the northern Brazilian Amazon. Forests, 10, art. 61.
1062   https://doi.org/10.3390/f10010061.

1063 Condé, T.M., Tonini, H., 2013. Fitossociologia de uma Floresta Ombrófila Densa na
1064   Amazônia Setentrional, Roraima, Brasil. Acta Amazonica, 43, 247–
1065   260. https://doi.org/10.1590/S0044-59672013000300002

1066 Crivelli, B.R.S., Gomes, J.P., Morais, W.W.C., Condé, T.M., Santos, R.L., Bonfim
1067   Filho, O.S., 2017. Caracterização do setor madeireiro de Rorainópolis, sul de
1068   Roraima. Revista Ciência da Madeira, 8(3), 142-150.
1069   https://doi.org/10.12953/2177-6830/rcm.v8n3p142-150.

1070 da Silva, S.S., Fearnside, P.M., Graça, P.M.L.A., Brown, I.F., Alencar, A., de Melo,
1071   A.W.F., 2018. Dynamics of forest fires in the southwestern Amazon. Forest
1072   Ecology and Management, 424, 312-322.
1073   https://doi.org/10.1016/j.foreco.2018.04.041.

1074 de Faria, B.L., Brando, P.M., Macedo, M.N., Panday, P.K., Soares-Filho, B.S., Coe,
1075   M.T., 2017. Current and future patterns of fire-induced forest degradation in
1076   Amazonia. Environmental Research Letters, 12(9), 1-13.
1077   https://doi.org/10.1088/1748-9326/aa69ce.

1078 Dent, B.D., Torguson, J., Hodler, T., 1990. Cartography: Thematic Map Design.
1079   Second edition. Dubuque, IA: William C. Brown. 448 pp.

1080   Fearnside, P.M., 1997. Wood density for estimating forest biomass in Brazilian
1081   Amazonia. Forest Ecology and Management, 90(1), 59-89.
1082   https://doi.org/10.1016/S0378-1127(96)03840-6

1083   Fearnside, P.M., 2003. Conservation policy in Brazilian Amazonia: Understanding the
1084   dilemmas. World Development, 31(5), 757-779. https://doi.org/10.1016/S0305-
1085   750X(03)00011-1.

1086   Fearnside, P.M., 2008. Amazon forest maintenance as a source of environmental
1087   services. Anais da Academia Brasileira de Ciências, 80, 101-114.
1088   https://doi.org/10.1590/S0001-37652008000100006.

1089   Fearnside, P.M., Barbosa, R.I., Pereira, V.B., 2013. Emissões de gases do efeito estufa
1090   por desmatamento e incêndios florestais em Roraima: Fontes e sumidouros.
1091   Revista Agroambiente On-line, 7, 95-111. https://doi.org/10.18227/1982-
1092   8470ragro.v7i1.971.

1093   Fernández-Manso, A., Fernández-Manso, O., Quintano, C., 2016. SENTINEL-2A red-
1094   edge spectral indices suitability for discriminating burn severity. International
1095   Journal of Applied Earth Observation and Geoinformation, 50, 170–175.
1096   https://doi.org/10.1016/j.jag.2016.03.005.

1097   Ferrante, L., Fearnside, P.M., 2019. Brazil's new president and "ruralists" threaten
1098   Amazonia's environment, traditional peoples and the global climate.
1099   Environmental Conservation, 46(4), 261-263.
1100   https://doi.org/10.1017/S0376892919000213.

1101   Fonseca, M.G., Anderson, L.O., Arai, E., Shimabukuro, Y.E., Xaud, H.A.M., Xaud,
1102   M.R., Madani, N., Wagner, F.H., Aragão, L.E.O.C., 2017. Climatic and
1103   anthropogenic drivers of northern Amazon fires during the 2015-2016 El Niño
1104   event. Ecological Applications, 27(8), 2514-2527.
1105   https://doi.org/10.1002/eap.1628.

1106   Fonseca, M.G., Alves, L.M., Aguiar, A.P.D., Arai, E., Anderson, L.O., Rosan, T.M.,
1107   Shimabukuro, Y.E., Aragão, L.E.O.C., 2019. Effects of climate and land-use
1108   change scenarios on fire probability during the 21st century in the Brazilian
1109   Amazon. Global Change Biology, 25(9), 2931-2946.
1110   https://doi.org/10.1111/gcb.14709.

1111   Ferrier, S., Ninan, K.N., Leadley, P., Alkemade, R., Acosta, L.A., Akçakaya, H.R.,
1112   Brotons, L., Cheung, W.W.L., Christensen, V., Harhash, K.A., Kabubo-Mariara,
1113   J., Lundquist, C., Obersteiner, M., Pereira, H.M., Peterson, G., Pichs-Madruga, R.,
1114   Ravindranath, N., Rondinini C., Wintle B.A. (Eds.), 2016. IPBES: The
1115   methodological assessment report on scenarios and models of biodiversity and
1116   ecosystem services. Bonn, Germany. Secretariat of the Intergovernmental Science-
1117   Policy Platform on Biodiversity and Ecosystem Services, 348 pp.
1118   https://ipbes.net/assessment-reports/scenarios.

1119   G1, 2018a. Protesto contra fechamento de madeireiras interdita rodovia em
1120   Rorainópolis, Sul de RR. Available at: https://bityl.co/7EMh. Accessed on: 26
1121   January 2021.

1122 G1, 2018b. PF faz operação de combate à exploração ilícita de madeira da Amazônia.
1123   Available at: https://bityl.co/5Jdo. Accessed on: 21 November 2020.

1124 Gimenez, B.O., Danielli, F.E., Oliveira, C.K.A., Santos, J., Higuchi, N., 2015.
1125   Equações volumétricas para espécies comerciais madeireiras do sul do estado de
1126   Roraima. Scientia Forestales, 43, 291-301.
1127   https://www.ipef.br/publicacoes/scientia/nr106/cap05.pdf.

1128 Hagen, A., 2003. Fuzzy set approach to assessing similarity of categorical maps.
1129   International Journal Geographical Information Science, 17, 235-249.
1130   https://doi.org/10.1080/13658810210157822.

1131 Hethcoat, M.G., Carreiras, J.M.B., Edwards, D.P., Bryant, R.G., Peres, C.A., Quegan,
1132   S., 2020. Mapping pervasive selective logging in the south-west Brazilian Amazon
1133   2000–2019. Environmental Research Letters, 15, art. 094057.
1134   https://doi.org/10.1088/1748-9326/aba3a4.

1135 Higuchi, N., Santos, J., Ribeiro, R.J., Minette L., Biot, Y., 1998. Biomassa da parte
1136   aérea da vegetação da floresta tropical úmida de terra-firme da Amazônia
1137   brasileira. Acta Amazonica, 28(2), 153-166. https://doi.org/10.1590/1809-
1138   43921998282166.

1139 Jiménez-Muñoz, J.C., Mattar, C., Barichivich, J., Santamaría-Artigas, A., Takahashi,
1140   K., Malhi, Y. et al., 2016. Record-breaking warming and extreme drought in the
1141   Amazon rainforest during the course of El Niño 2015-2016. Scientific Reports, 6,
1142   1–7. https://doi.org/10.1038/srep33130.

1143 Leite-Filho, A.T., Soares-Filho, B.S., Davis, J.L., Abrahão, G.M., Börner, J., 2021.
1144   Deforestation reduces rainfall and agricultural revenues in the Brazilian Amazon.
1145   Nature Communications, 12, art. 2591. https://doi.org/10.1038/s41467-021-22840-
1146   7.

1147 Lentini, M., Pereira, D., Celentano, D., Pereira, R., 2005. Fatos florestais da Amazônia
1148   2005. Belém, PA, Brazil: Instituto do Homem e Meio Ambiente da Amazônia
1149   (Imazon). 140 pp. https://bityl.co/5JdR

1150 Marcelino, E.V., 2008. Desastres Naturais e Geotecnologias: Conceitos Básicos.
1151   Caderno Didático nº 1. Santa Maria, RS, Brazil: CRS, Instituto Nacional de
1152   Pesquisas Espaciais (INPE), 38 pp. https://bityl.co/5JdF

1153 McLauchlan, K.K., Higuera, P.E., Miesel, J., Rogers, B.M., Schweitzer, J., Shuman,
1154   J.K., Tepley, A.J., Varner, J.M., Veblen, T.T., Adalsteinsson, S.A. et al., 2020.
1155   Fire as a fundamental ecological process: Research advances and frontiers. Journal
1156   of Ecology, 108(5), 2047-2069. https://doi.org/10.1111/1365-2745.13403.

1157 Meira-Junior, M.S., Pinto, J.R.R., Ramos, N.O., Miguel, E.P., Gaspar, R.O., Phillips,
1158   O.L., 2020. The impact of long dry periods on the aboveground biomass in a
1159   tropical forest: 20 years of monitoring. Carbon Balance and Management, 15, art.
1160   12. https://doi.org/10.1186/s13021-020-00147-2.

1161 Monteiro, A., Cardoso, D., Conrado, D., Veríssimo, A., Souza Jr, C., 2010. Boletim
1162   Transparência Manejo Florestal- Estado do Pará 2008 a 2009. Belém, PA, Brazil:
1163   Instituto do Homem e Meio Ambiente da Amazônia (Imazon), 16 pp.
1164   https://bityl.co/5Jd4

1165 Morton, D.C., DeFries, R.S., Nagol, J., Souza Jr., C.M., Kasischke, E.S., Hurtt, G.C.,
1166   Dubayah, R., 2011. Mapping canopy damage from understory fires in Amazon
1167   forests using annual time series of Landsat and MODIS data. Remote Sensing of
1168   Environment, 115(7), 1706-1720. https://doi.org/10.1016/j.rse.2011.03.002.

1169 Nascimento, M.T., Carvalho, L.C.S., Barbosa, R.I., Villela, D.M., 2014. Variation in
1170   floristic composition, demography and above-ground biomass over a 20-year
1171   period in an Amazonian monodominant forest. Plant Ecology and Diversity, 7 (1–
1172   2), 293–303. https://doi.org/10.1080/17550874.2013.772673

1173 Nepstad, D.C., Veríssimo, A., Alencar, A., Nobre, C., Lima, E., Lefebvre, P. ,
1174   Schlesinger, P., Potter, C., Moutinho, P., Mendoza, E., Cochrane, M., Brooks, V.
1175   1999. Large-scale impoverishment of Amazonian forests by logging and fire.
1176   Nature, 398, 505-508. https://www.nature.com/articles/19066.

1177 Nepstad, D., Lefebvre, P., Lopes da Silva, U., Tomasella, J., Schlesinger, P.,
1178   Solorzano, L., Moutinho, P., Ray, D., Guerreira Benito, J., 2004. Amazon drought
1179   and its implications for forest flammability and tree growth: A basin-wide
1180   analysis. Global Change Biology, 10(5), 704-717. https://doi.org/10.1111/j.1529-
1181   8817.2003.00772.x

1182 Nepstad, D.C., Tohver, I.M., Ray, D., Moutinho, P., Cardinot, G., 2007. Mortality of
1183   large trees and lianas following experimental drought in an Amazon forest.
1184   Ecology, 88(9), 2259-2269. https://doi.org/10.1890/06-1046.1.

1185 Nogueira, E.M., Nelson, B.W., Fearnside, P.M. 2005. Wood density in dense forest in
1186   central Amazonia, Brazil. Forest Ecology and Management, 208, 261-286.
1187   https://doi.org/10.1016/j.foreco.2004.12.007

1188 Nogueira, E.M., Fearnside, P.M., Nelson, B.W., Barbosa, R.I., Keizer, E.W.H., 2008.
1189   Estimates of forest biomass in the Brazilian Amazon: New allometric equations
1190   and adjustments to biomass from wood-volume inventories. Forest Ecology and
1191   Management, 256, 1853-1857. https://doi.org/10.1016/j.foreco.2008.07.022

1192 Nunes J.C., 2018. Ibama apreende 7 mil toras de madeira extraídas ilegalmente da
1193   Terra Indígena Piritити. Radioagência Nacional, 2 May 2018. https://bityl.co/5K63

1194 Oliveira, S., 2021. Rorainópolis, em RR, entra na lista de municípios com prioridade
1195   no controle ao desmatamento na Amazônia. G1, 13 January 2021. Available at:
1196   https://bityl.co/5Jdh. Accessed on: 15 January 2021.

1197 Pereira, D., Santos, D., Vedoveto, M., Guimarães, J., Veríssimo, A., 2010. Fatos
1198   florestais da Amazônia. Belém, PA: Instituto do Homem e Meio Ambiente da
1199   Amazônia (Imazon), 124 pp. https://bityl.co/5Jd6

1200 Quintano, C., Fernández-Manso, A., Fernández-Manso, O., Shimabukuro, Y.E., 2006.
1201   Mapping burned areas in Mediterranean countries using spectral mixture analysis
1202   from a uni-temporal perspective. International Journal of Remote Sensing, 27,
1203   645-662. https://doi.org/10.1080/01431160500212195

1204 Rappaport, D.I., Keller, M., Morton, D.C., Longo, M., Dubayah, R., Dos-Santos,
1205   M.N., 2018. Quantifying long-term changes in carbon stocks and forest structure
1206   from Amazon forest degradation, Environmental Research Letters, 13(6). 1-12.
1207   https://iopscience.iop.org/article/10.1088/1748-9326/aac331.

1208 Ray, D., Nepstad, D., Moutinho, P., 2005. Micrometeorological and canopy controls
1209   of fire susceptibility in a forested Amazon landscape. Ecological Society of
1210   America, 15, 1664-1678. https://doi.org/10.1890/05-0404

1211 Silva, C.V.J., Aragão, L.E.O.C., Barlow, J., Espirito-Santo, F., Young, P.J, Anderson,
1212   L.O., Berenguer, E., Brasil, I., Brown, I.F., Castro, B., Farias, R. et al., 2018.
1213   Drought-induced Amazonian wildfires instigate a decadal scale disruption of
1214   forest carbon dynamics. Philosophical Transactions of the Royal Society B, 373,
1215   art. 20180043. https://doi.org/10.1098/rstb.2018.0043.

1216 Silveira, L.H.C., Rezende, A.V., Vale, A.T., 2013. Teor de umidade e densidade
1217   básica da madeira de nove espécies comerciais amazônicas. Acta Amazonica,
1218   43(2), 179–184. https://doi.org/10.1590/S0044-59672013000200007

1219 Silvestrini, R.A., Soares-Filho, B.S., Nepstad, D., Coe, M., Rodrigues, H., Assunção,
1220   R., 2011. Simulating fire regimes in the Amazon in response to climate change
1221   and deforestation. Ecological Applications, 21, 1573–1590.
1222   https://doi.org/10.1890/10-0827.1

1223 Slocum, T.A., 1999. Thematic Cartography and Visualization. Upper Saddle River,
1224   NJ, USA: Prentice Hall.

1225 Soares-Filho, B.S., Nepstad, D.C., Curran, L., Cerqueira, G.C., Garcia, R.A., Ramos,
1226   C.A., Voll, E., Mcdonald, A., Lefebvre, P., Schlesinger, P., 2006. Modelling
1227   conservation in the Amazon basin. Nature, 440, 520-523.
1228   https://doi.org/10.1038/nature04389

1229 Soares-Filho, B.S., Garcia, R.A., Rodrigues, H., Moro, S., Nepstad, D., 2008. Nexos
1230   entre as dimensões socioeconômicas e o desmatamento: A caminho de um modelo
1231   integrado. In: Batistella, M., Alves, D., Moran, E. (Eds.). Amazônia. Natureza e
1232   Sociedade em Transformação. v. 1., São Paulo, SP, Brazil: EDUSP.
1233   https://bityl.co/5Ji4

1234 Souza Jr., C.M., Roberts, D., Monteiro, A.L., 2005a. Multitemporal analysis of
1235   degraded forests in the southern Brazilian Amazon. Earth Interactions, 9, art. 19.
1236   https://doi.org/10.1175/EI132.1

1237 Souza Jr., C.M., Roberts, D., Cochrane, M.A. 2005b. Combining spectral and spatial
1238   information to map canopy damages from selective logging and forest fires.
1239   Remote Sensing of Environment, 98, 329-343.
1240   https://doi.org/10.1016/j.rse.2005.07.013.

1241 Souza, Jr, C.M., Siqueira, J.V., Sales, M.H., Fonseca, A.V., Ribeiro, J.G., Numata, I.,
1242   Cochrane, M.A., Barber, C.P., Roberts, D.A., Barlow, J., 2013. Ten-year Landsat
1243   classification of deforestation and forest degradation in the Brazilian Amazon.
1244   Remote Sensing, 5(11), 5493-5513. https://doi.org/10.3390/rs5115493.

1245 Stark, S.C., Breshears, D.D., Aragón, S., Villegas, J.C., Law, D.J., Smith, M.N.,
1246   Minor, D.M., de Assis, R.L., de Almeida, D.R.A., de Oliveira, G., Saleska, S.R.,
1247   Swann, A.L.S., Moura, J.M.S., Camargo, J.L., da Silva, R., Aragão, L.E.O.C.,
1248   Oliveira. R.C., 2020. Reframing tropical savannization: Linking changes in
1249   canopy structure to energy balance alterations that impact climate. Ecosphere,
1250   11(9), art. e03231. https://doi.org/10.1002/ecs2.3231.

1251   Stroppiana D., Bordogna, G., Carrara, P., Boschetti, M., Boschetti, L., Brivio; P.A.
1252   2012. A method for extracting burned areas from Landsat TM/ETM+ images by
1253   soft aggregation of multiple Spectral indices and a region growing algorithm.
1254   ISPRS Journal of Photogrammetry and Remote Sensing, 69(1), 88-102.
1255   https://doi.org/10.1016/j.isprsjprs.2012.03.001

1256   Trumbore, S., Brando, P., Hartmann, H., 2015. Forest health and global change.
1257   Science, 349, 814-818. https://doi.org/10.1126/science.aac6759

1258   Turubanova, S., Potapov, P.V., Tyukavina, A., Hansen, M.C., 2018. Ongoing primary
1259   forest loss in Brazil, Democratic Republic of the Congo, and Indonesia.
1260   Environmental Research Letters, 13, art. 074028. https://doi.org/10.1088/1748-
1261   9326/aacd1c.

1262   Uhl, C., Buschbacher, R., 1985. A disturbing synergism between cattle-ranch burning
1263   practices and selective tree harvesting in the eastern Amazon. Biotropica, 17(4),
1264   265-268. https://doi.org/10.2307/2388588

1265   USGS (U.S. Geological Survey), 2016. U.S. Department of the Interior, USGS.
1266   Available at: http://earthexplorer.usgs.gov/. Accessed on: 20 October 2016.

1267   Watson, J.E.M., Evans, T., Venter, O., Williams, B., Tulloch, A., Stewart, C.,
1268   Thompson, I., Ray, J.C., Murray, K., Salazar, A. et al., 2018. The exceptional
1269   value of intact forest ecosystems. Nature Ecology & Evolution, 2, 599–610.
1270   https://doi.org/10.1038/s41559-018-0490-x

1271   West, T.A.P., Fearnside, P.M., 2021. Brazil's conservation reform and the reduction of
1272   deforestation in Amazonia. Land Use Policy, 100, art. 105072.
1273   https://doi.org/10.1016/j.landusepol.2020.105072

1274   Xaud, H.A.M., Martins, F.S.R.V., Santos, J.R., 2013. Tropical forest degradation by
1275   mega-fires in the northern Brazilian Amazon. Forest Ecology and Management,
1276   294, 97-106. https://doi.org/10.1016/j.foreco.2012.11.036

1277   Ziccardi, L.G., Graça, P.M.L.A., Figueiredo, E.O., Fearnside, P.M., 2019. Decline of
1278   large-diameter trees in a bamboo-dominated forest following anthropogenic
1279   disturbances in southwestern Amazonia. Annals of Forest Science, 76, art. 110.
1280   https://doi.org/10.1007/s13595-019-0901-4

Supplementary material

Logging Amazon forest increased the severity and spread of fires during the 2015-2016 El Niño

Paulo Eduardo Barni [1]
Anelícia Cleide Martins Rego [2]
Francisco das Chagas Ferreira Silva [2]
Richard Anderson Silva Lopes[3]
Haron Abrahim Magalhães Xaud [4]
Maristela Ramalho Xaud [4]
Reinaldo Imbrozio Barbosa [5]
Philip Martin Fearnside [6]

[1] Professor da Universidade Estadual de Roraima – UERR, *Campus* Rorainópolis
Av. Senador Helio Campos, s/nº, 69375-000, Rorainópolis, Roraima, Brazil.
pbarni@uerr.edu.br

[2] Graduados da Universidade Estadual de Roraima – UERR, *Campus* Rorainópolis
Av. Senador Helio Campos, s/nº, 69375-000, Rorainópolis, Roraima, Brazil.
{anelycia.com@gmail.com; chagasferreirasilva@gmail.com}

[3] Corpo de Bombeiros Militares de Roraima, Coordendoria Estadual de Proteção e Defesa Civil. Avenida Venezuela, 1271, 69309690 - Boa Vista, Roraima, Brazil.
{raslopes@gmail.com}

[4] Empresa Brasileira de Pesquisa Agropecuária – Embrapa/RR. Rodovia BR 174, Km 8, Distrito Industrial. 69301-970, Boa Vista, Roraima, Brazil. {haronxaud@gmail.com; marisxaud@gmail.com}

[5] Instituto Nacional de Pesquisas da Amazônia (INPA), Rua Coronel Pinto, 315. CEP: 69301-150. Boa Vista, Roraima, Brazil. reinaldo@inpa.gov.br

[6] Instituto Nacional de Pesquisas da Amazônia (INPA), Av. André Araújo, 2936. CEP: 69067-375, Manaus, Amazonas, Brazil. pmfearn@inpa.gov.br

Supplementary material index:

1. Methodological procedures
1.1 Study area

Most of the study area (6402.6 km^2, or 96.2% of the study area) is in the municipality of Rorainópolis, followed by the municipality of São Luiz (164.2 km^2, or 2.4%) and the municipality of Caracaraí (90.5 km^2, or 1.4 %) (Table S1).

Table S1. Deforestation, forest fire, and logging in the portion of each municipality located in the study area.

Municipalities	Area (km^2)	% of the study area	Deforestation km^2	%	Forest fire (km^2)	% of the burned area	SL (km^2)	% of the logged area
Caracaraí	90.5	1.4	7.1	0.6	37.9	5.6	9.4	1.5
Rorainópolis	6,402.6	96.2	1,045.3	94.8	638.3	93.6	624.4	96.8
São Luiz	164.2	2.4	49.7	4.5	6.0	0.9	10.9	1.7
Total	**6,657.3**	**100.0**	**1,102.1**	**100.0**	**682.2**	**100.0**	**644.8**	**100.0**

1.2 Forest inventory locations

The locations and other information for plots sampled in the field are presented in Table S2. All plots measured 4×250 m (1000 m^2).

Table S2. Location (latitude and longitude), area (ha) and date of field data collection. SL=Selective Logging. Wo-SL = without selective logging. W-SL = with selective logging.

Plot name	SL	Latitude	Longitude	Area (ha)	*AGB_stock (Mg ha^{-1})	Fire	Census date (mm/dd/yyyy)
Plot 1	W-SL	0.930891	-60.451279	0.1	404.6	yes	03/11/2016
Plot 2	W-SL	0.932695	-60.447959	0.1	221.5	yes	03/11/2016
Plot 3	W-SL	0.929629	-60.442604	0.1	458.5	yes	03/16/2016
Plot 4	W-SL	0.927556	-60.441827	0.1	322.0	yes	03/16/2016
Plot 5	W-SL	0.934315	-60.449995	0.1	640.2	yes	03/16/2016
Plot 6	W-SL	0.934234	-60.452384	0.1	834.0	yes	03/16/2016
Plot 7	W-SL	0.909708	-60.452814	0.1	320.1	yes	03/23/2016
Plot 8	W-SL	0.906816	-60.453078	0.1	567.2	yes	03/23/2016
Plot 9	W-SL	0.912540	-60.452564	0.1	1095.4	yes	03/23/2016
Plot 10	W-SL	0.913743	-60.454606	0.1	427.1	yes	03/23/2016
Plot 11	W-SL	0.711231	-60.565005	0.1	863.9	yes	03/30/2016
Plot 12	Wo-SL	0.707785	-60.510418	0.1	289.6	yes	03/30/2016
Plot 13	Wo-SL	0.709255	-60.508096	0.1	504.0	yes	03/30/2016
Plot 14	W-SL	0.709511	-60.567284	0.1	1044.2	yes	03/30/2016
Plot 15	W-SL	0.712057	-60.587902	0.1	387.6	yes	03/30/2016
Plot 16	W-SL	0.712389	-60.591582	0.1	424.0	yes	03/30/2016
Plot 17	Wo-SL	0.989933	-60.425055	0.1	546.6	yes	04/06/2016
Mean	-	-	-	-	**550.0**	-	-

*Aboveground dry biomass stock based on Higuchi et al. (1998) with adjustment for 40% water content (Higuchi et al., 1998) and for biomass of palms (Saldarriaga et al., 1988).

1.3 Biomass calculation in inventory plots for deriving fractions of biomass killed

Unlike the biomass map for Roraima, which used the Barni et al. (2016) analysis with species specific data, only about half of the trees in the plots had known identities, and we therefore used the Higuchi et al. (1998) equation to calculate fresh biomass directly from DBH without using species-specific wood-density data. Because the plot data are only used for deriving the fractions of biomass killed by the fire in the different severity classes, not the forest

biomass to which these fractions will be applied, the use of different biomass estimation equations will not affect the results for the impact of fire in the study area, since the both the numerator and the dominator in the fractions of biomass killed have been calculated with the same method.

Fresh weight was converted to dry weight by multiplying by 0.60, which was the dry weight to fresh weight ratio derived by Higuchi et al. (1998: Table 3b). This rate was applied to the fresh-biomass value calculated by the Higuchi et al. (1998) equation for each tree in the database. This procedure was performed from the excel spreadsheet. Thus:

$$Ln(Fresh\ weight) = -1.497 + 2.548 \times Ln(DBH)$$
$$Dry\ weight = EXP(Ln\ (Fresh\ weight)) \times 0.6$$

The total weight (kg^{-1}) of each plot (sum of the dry weight of all trees in the plot) was multiplied by 10 (to transform from kg^{-1} per plot to $kg\ ha^{-1}$) and, in sequence, the total weight in $kg\ ha^{-1}$ was divided by 1000 to transform into $Mg\ ha^{-1}$.

1.4 Area (ha) and volume (m^3) authorized in "alternative land-use" projects

The largest area authorized for deforestation (3300.7 ha, or 26.4% of the total area authorized) was in 2015 and the smallest (290.6 ha, or 2.3%) was in 2011. Only 26.2% (3114.1 ha) of these areas authorized for alternative land use were effectively deforested by 2019 (Table S3).

Table S3. Area and volume of wood authorized for harvest in alternative land-use projects in the study area.

Year	n	Authorized area (ha)	Authorized volume (m^3)	Average volume ($m^3\ ha^{-1}$)	*Deforestation (ha)	%	**YARSL (n)
2010	9	2,095.4	133,939.0	63.7	525.9	25.1	2.8
2011	2	290.6	13,027.8	49.5	102.4	35.2	4
2012	17	3,244.9	150,319.5	50.6	755.5	23.3	2
2013	4	873.2	46,156.7	53.3	195.0	22.3	1
2014	12	2,676.1	114,311.9	43.0	695.8	26.0	1
2015	14	3,300.7	153,920.6	48.4	839.7	25.4	4
Total	**58**	**12,480.9**	**611,675.5**	**51.4**	**3114.1**	**26.2**	**2.5**

* Deforestation by 2019.
** Years after the release to SL.

1.5 "Sustainable Forest Management" Plans

The areas released for selective logging in "sustainable forest management" plans in Rorainópolis totaled 11,958.8 ha from 2016 to 2020 with an average authorized harvest of 23.9 $m^3\ ha^{-1}$. In this area, a total volume of 281,091.3 m^3 of wood in logs was released (Table S4).

Table S4. Location (latitude and longitude), area (ha) and volume (m^3) authorized for logging in "sustainable forest management" plans in the municipality of Rorainópolis.

ID	Latitude	Longitude	Authorized area (ha)	Authorized volume (m^3)	Average volume (m^3 ha^{-1})	Year
1	0.4351889	-60.4069556	552.6	13,079.7	23.7	2019/20
2	0.3815278	-60.6354444	957.9	14,712.8	15.4	2017/18
3	0.5415483	-60.4245542	1,442.9	35,830.9	24.8	2019/20
4	0.7514861	-60.6653361	1,254.1	19,664.6	15.7	2018/19
5	0.5598333	-60.3416111	1,071.0	22,125.1	20.7	2018/19
6	0.7100000	-60.0663889	987.9	26,066.4	26.4	2016/17
7	0.5574109	-60.6592349	964.3	24,456.3	25.4	2020/21
8	0.2734927	-60.4002495	1,163.9	33,588.1	28.9	2020/21
9	0.5218820	-60.6587190	947.7	22,580.0	23.8	2020/21
10	0.9931272	-60.5705950	192.6	5.570.0	28.9	2020/21
11	0.2588300	-60.4437717	1,089.9	31,847.2	29.2	2020/21
12	0.4905078	-60.3520806	666.4	17,003.1	25.5	2020/21
13	0.4905078	-60.3520806	667.8	14,567.1	21.8	2020/21
	Total		**11,958.8**	**281,091.3**	**23.9**	

1.6 Fire severity estimation by NDVI and NBR

The results of the comparison between NDVI and NBR using fire-severity classes (light, moderate, strong and very strong) are presented in Table S5. Figure S1 shows the results of the comparative analysis between the NDVI and the NBR in the assessment of burned areas. Figure S2 shows a portion of the study area with fire-severity classifications by each index.

The larger area that the NBR index detected in the lowest severity class (light), as compared to NDVI, is an indication in favor of NDVI as a more accurate index for our purposes. The fires in the area occurred from 1 December 2015 to 23 March 2016, with most of the 216 "hot pixels" detected by the Aqua satellite being detected between 15 January and 5 February 2016. This means that the bulk of the burning was almost five months before the satellite pass on 9 June 2016, and, with the rainy season beginning at the end of March, there were over two months of rain before the satellite pass. Therefore there had been time for regeneration of green vegetation in the understory of the burned areas. The burn-severity classification by the sensors would be most likely to downgrade the assignment of values in lower severity classes, such as classifying a "moderate" burn as "light," because the more-severe burns would inhibit regeneration. The close agreement between the two indices (9,6% NDVI and 8.6% NBR) in their findings for the highest severity class (very strong) can be explained by the almost total inhibition of regeneration in these places when fire is very intense. In this case, the intensity of the fire may have partially or totally eliminated the seed bank from the soil, thereby making more time necessary for regeneration (Figure S2).

NDVI and NBR use different bands, which may have made the green regeneration lead NBR to downgrade the assigned severities more than did NDVI. NDVI uses Landsat 8 sensor bands 5 (near infrared [NIR] wavelength range: 0.851 - 0.879 micrometers) and 4 (red: 0.636 - 0.673 micrometers). NBR uses bands 7 (short-wave infrared 2 [SWIR2]: 2.107 – 2.294 micrometers) and 5 (NIR: 0.851 - 0.879 micrometers). In the case of NBR, there is an increase in the contrast between the values of photosynthetically active vegetation and photosynthetically inactive vegetation (dead biomass). Higher reflectance levels associated with photosynthetically active vegetation, and part of this increase in "greenness" detected by NBR, can be attributed to forest regeneration by sprouting, seedling emergence from the soil seed bank and appearance of herbaceous plants in abundance.

Both indices capture the "greenness" effect, but this reflection is not very evident in the case of NDVI because this composition uses band 4 (red). When using band 7 to compose the NBR there is a greater expansion of the values due to the greater contrast (greater difference) between the reflection values of bands 5 and 7 than between the reflection values of bands 5 and 4 used to compose the NDVI. For example, in our study the range of the NBR index values was 0.5010 (0.7205 minus 0.2104: Table S5) while the range of the NDVI was 0.3784 (0.6031 minus 0.2247: Table 1 in the main text). This difference meant a 32.4% increase in the amplitude of the NBR values in relation to the amplitude of the NDVI values.

This explanation is speculative due to the lack of information linking ground-level regeneration with the NBR index. Our empirical experience suggests rapid regeneration in lower-severity burns. This subject should be the object of future studies in the region due to the importance of improving forest degradation estimates.

Table S5. Comparison analysis between NDVI and NBR using fire-severity classes.

Class	NDVI Area (km^2)	NDVI %	NBR Area (km^2)	NBR %	NDVI-NBR Area (km^2)	NDVI-NBR %	NBR values Dimensionless (- 1 to +1)
Light	245.8	36.2	282.9	41.7	-37.1	-15.1	0.5764 to 0.7205
Moderate	227.5	33.5	206.9	30.5	20.6	9.1	0.4904 to 0.5764
Strong	140.2	20.7	130.2	19.2	10.0	7.1	0.3944 to 0.4904
Very strong	64.8	9.6	58.3	8.6	6.5	10.0	0.2104 to 0.3944
Total	**678.3**	**100.0**	**678.3**	**100.0**	**0.0**	**-**	**-**
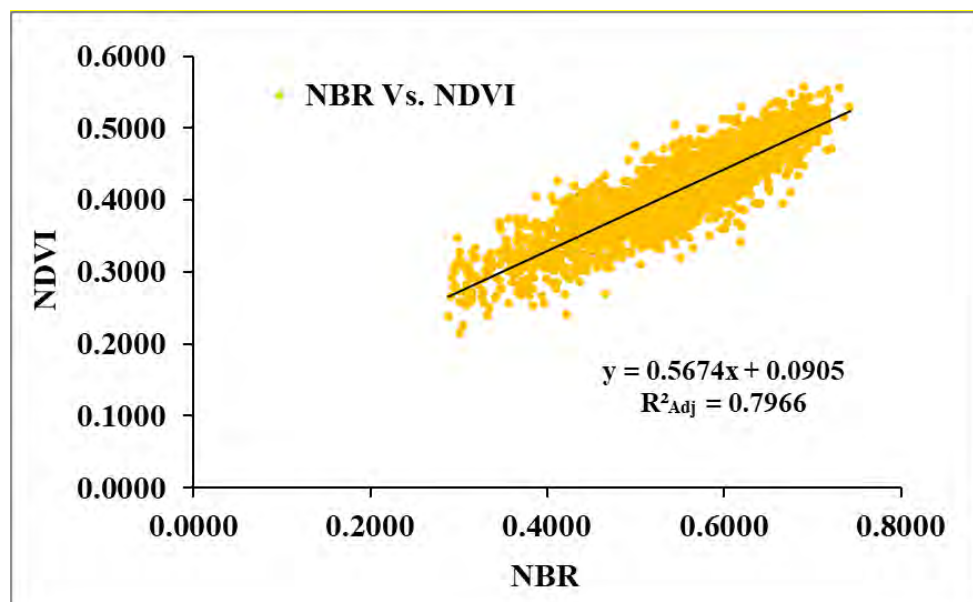
Figure S1. Comparison between sample values (n = 2502) for NBR and NDVI in burned areas in the study area.
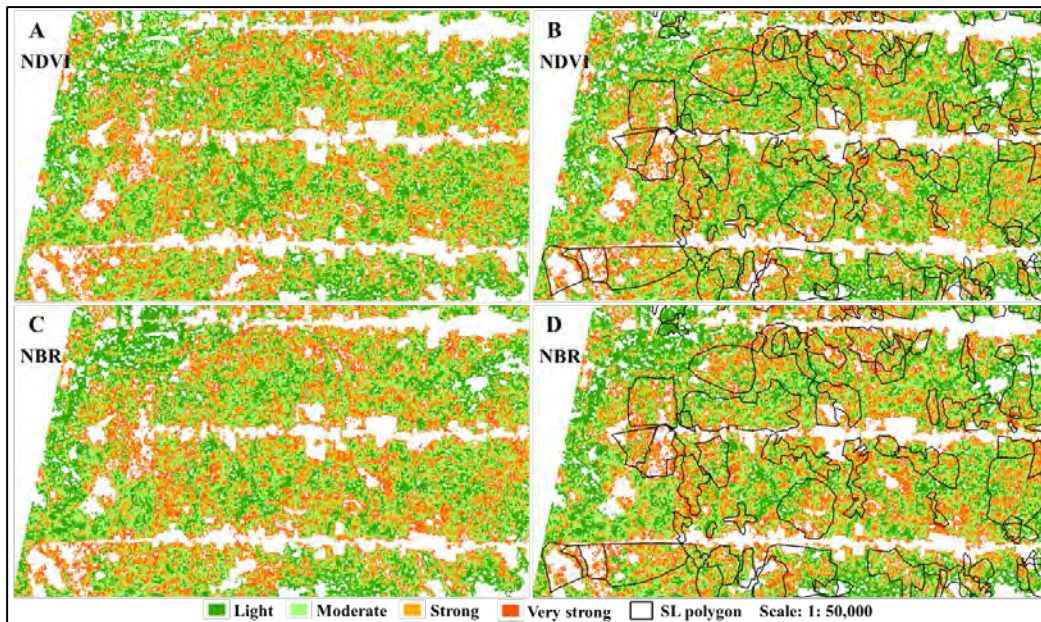
Figure S2. Fire severity classification using NDVI (A and B) and NBR (C and D) in a portion of the study area.

1.7 Wood density

The values calculated for the basic density of wood (g cm^{-3}) harvested in the SL areas are shown in Table S6. The table also provides the sources of the information.

Table S6. Calculation of weighted mean wood density.

Species	Local name	Wood volume (1)		Basic density	Note	Weighted	Density
		m³	%	(g cm^{-3})			Source
Manilkara huberi	Maçaranduba	9,806	29.2	0.878	(2)	0.257	Silveira et al., 2013
Dinizia excelsa	Angelim-ferro	9,235	27.5	0.86		0.237	Fearnside, 1997
Hymenolobium excelsum	Angelim-pedra	4,440	13.2	0.64		0.085	Fearnside, 1997
Goupia glabra	Cupiúba	3,880	11.6	0.712	(2,3)	0.082	Nogueira et al., 2005
Erisma fuscum	Caferana	2,170	6.5	0.49	(4)	0.032	Fearnside, 1997
Qualea paraensis	Rabo-de-arraia	1,350	4.0	0.67		0.027	Fearnside, 1997
Protium sp.	Casca-grossa	1,000	3.0	0.589	(2,3,5)	0.018	Nogueira et al., 2005
Clarisia racemosa	Guaruba	1,000	3.0	0.665	(2)	0.020	Silveira et al., 2013
Couratari stellata	Tauari	320	1.0	0.63		0.006	Fearnside, 1997
Bagassa guianensis	Tatajuba	280	0.8	0.69		0.006	Fearnside, 1997
Handroanthus sp.	Ipê	77	0.2	0.91		0.002	Fearnside, 1997

(1) Wood volumes are from a 2013 survey of 9 sawmills in Rorainópolis by Crivelli et al., 2017).
(2) Includes variation along the trunk.
(3) Includes radial variation (density of cross-sectional discs, including bark)
(4) Density of a congeneric.
(5) Mean of 14 trees from 7 species.

1.8 Estimation of harvesting intensity and loss of live biomass from cumulative selective logging by 2015

Only an approximate value can be estimated for the loss of live biomass to selective logging at the time of the 2015-2016 fires. Official data on log volumes processed in sawmills and

authorized for sale have wide discrepancies, and data are only available for certain years for different measures (Table S7). The data for log volume processed in sawmills, which information is available for the most years (2007-2019) is particularly unreliable. From 2007 to 2014 the volume officially reported (Brazil, IBGE, 2021) averaged 34,525 m³ year⁻¹, jumping by 5.3 fold in 2015 to a new level, presumably due to an improvement in the veracity of reporting beginning in 2015. The new level presumed to originate in the municipality of Rorainópolis (90%, see text) is close (4.5% below) to the amount authorized for sale from clearcutting projects in 2015, the only year with data on the clearcutting projects after this shift (data on clearcutting projects are available for 2010-2015). The volume data for clearcutting authorizations therefore appears to be a good representation of the portion (estimated at 90%) of volume processed by sawmills in Rorainópolis that originates within the municipality and therefore in the 520.5-km² area where we mapped selective logging. During the 6 years with data for authorizations of clearcutting projects (2010-2015) the mean amount authorized was 101,945.8 m³ year⁻¹. From this 1.2% must be deducted for the logs that were sold from the areas that were authorized for clearcutting that were, in fact, actually clearcut (see text), meaning that the volume harvested through selective logging was 100.742.5 m³ year⁻¹. If one considers that this annual harvest also applies to the preceding 4 years (2006-2009), when substantial logging activity is known to have taken place, then the harvest intensity considering the 10-year 2006-2015 period was 19.4 m³ ha⁻¹. Considering the mean basic density the wood of 0.770 (See text Section 2.3.2), this removal in logs represents 14.9 Mg ha⁻¹. To obtain the reduction in live biomass from the selective logging we must also include the stumps and crowns of the harvested trees, as well as the biomass of unharvested trees killed from damage in the logging operations. Nogueira et al. (2008) found that stumps represented 1% of the biomass of the commercial boles in 264 harvested trees in Brazil's "arc of deforestation" in the southern part of Brazilian Amazonia. Applying this percentage, the stumps represent 0.15 Mg ha⁻¹, and the trunk from the ground to the first significant branch for the harvested trees represents 15.05 Mg ha⁻¹. Crowns were found to represent an average of 30.8% of the aboveground biomass in 121 trees in dense forest near Manaus (da Silva, 2007, p. 57). The crowns of the harvested trees therefore represent 6.7 Mg ha⁻¹, and the total (commercial log + stump + crown) represents 21.75 Mg ha⁻¹. Since this illegal selective logging does not employ reduced-impact techniques, damage equal to 64% of the harvested biomass is considered, based on studies reviewed in Fearnside (1995, p. 321). This increases the aboveground biomass loss to 35.67 Mg ha⁻¹.

Table S7. Comparison of official data sources on log volumes in Rorainópolis

Year	Volume processed in sawmills (m³) (a)	Processed log volume assumed to come from Rorainópolis (m³) (b)	Volume authorized in deforestation projects (m³) (c)	Volume authorized in forest-management projects (m³) (d)	Discrepancy between processed volume assumed to come from Rorainópolis and volume authorized in deforestation projects (m³)	(%)
2007	40,000	36,000				
2008	32,700	29,430				
2009	32,500	29,250				
2010	33,000	29,700	133,939.0		104,239.0	351.0
2011	32,600	29,340	13,027.8		-16,312.2	-55.6
2012	35,000	31,500	150,319.5		118,819.5	377.2
2013	36,400	32,760	46,156.7		13,396.7	40.9
2014	34,000	30,600	114,311.3		83,711.3	273.6
2015	179,147	161,232	153,920.6		-7,311.7	-4.5
2016	193,210	173,889		20,066.4		
2017	424,601	382,141		14,712.8		
2018	155,942	140,348		41,789.7		
2019	170,000	153,000		13,079.7		
2020				149,611.8		
2010-2015		315,132.3	611,674.9		296,542.6	94.1
2010-2014		153,900	457,754.0		303,854.3	197.4

(a) Brazil, IBGE (2021).
(b) Assumed 90% originates from the municipality of Rorainópolis and 10% from the neighboring municipality of Caracaraí and São Luiz. Volume from indigenous areas is assumed not to be reported.
(c) Table S3.
(d) Table S4.

1.9 Selective logging
1.9.1 Mapping of the selective logging

For mapping selective logging, 16 images were used: 10 images from Landsat 5 TM and six from Landsat 8 OLI / TIRS (Table S8). The classification was checked by field observations in burned and unburned areas in 21 inventoried plots after the fires occurred (Barni et al., 2017), of which 17 were used in the present study. We also used a vector file (shapefile) provided by FEMARH for areas licensed for deforestation (128.3 km²) in our study area during the same period of analysis (2007 to 2015) as a way to resolve doubts about spectral patterns in the images caused by SL. After mapping SL for this interval, the vector files were gathered in a single vector layer, converting this to an SL map (Figure S3).

Table S8. Mapping of selective logging (SL) from 2007 to 2015 in the study area.

*Year	**Image date	**Satellite data	SL (km²)	%	***Deforestation (km²)	%
2007	21 Sept.	Landsat 5	39.7	6.2	19.4	11.3
2008	10 Nov.	Landsat 5	37.6	5.8	26.3	15.3
2009	29 Nov.	Landsat 5	46.9	7.3	18.2	10.6
2010	15 Oct.	Landsat 5	75.9	11.8	16.1	9.3
2011	31 Aug.	Landsat 5	80.4	12.5	11.2	6.5
2012	–	–	–	–	15.5	9.0
2013	23 Oct.	Landsat 8	72.4	11.2	22.8	13.2
2014	29 Dec.	Landsat 8	93.1	14.4	19.5	11.3
2015	30 Nov.	Landsat 8	198.7	30.8	23.3	13.5
TOTAL	16	–	644.8	100.0	172.3	100.0

* No images were observed for the year 2012 in our study area.
** RGB and NDVI images.
*** Deforestation in the municipality of Rorainópolis (Brazil, INPE, 2020).
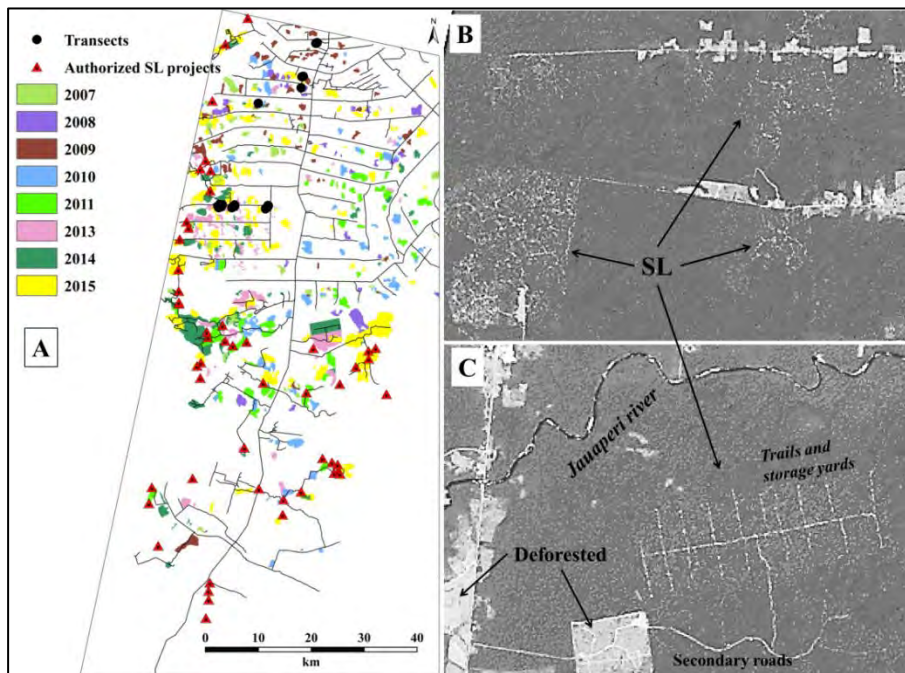
Figure S3. (A) Selective-logging map from 2007 to 2015 with the location of the 17 transects from the forest inventory and SL projects authorized by FEMARH in the study area, and in (B) and (C) detection of the SL areas in the RGB and NDVI images (Scale: 1: 50,000).

1.9.2 Severity of fire according to the year of selective logging

Analysis of the fire severity classes in areas impacted by SL showed that the class with the greatest severity ("very strong") increased with decreasing time elapsed between the harvesting of wood and the occurrence of the fire. For example, for areas logged in 2007 the difference between the "light" and "very strong" classes was 7.4%, while for areas logged in 2015 (the year the fire started in the region) this difference was ~ 3 times greater (21.9%) (Table S9).

Table S9. Severity of fire according to the year of selective logging

Year	Light Area (km²)	%	Moderate Area (km²)	%	Strong Area (km²)	%	Very strong Area (km²)	%	Total
2007	5.5	10.8	6.1	10.4	4.5	10.0	3.0	11.6	**19.1**
2008	3.3	6.4	3.0	5.2	1.9	4.2	0.8	2.9	**8.9**
2009	7.1	13.9	7.6	13.0	4.8	10.5	2.1	8.1	**21.5**
2010	6.0	11.8	5.0	8.7	2.7	6.0	0.9	3.6	**14.7**
2011	3.7	7.2	4.0	6.9	2.9	6.4	1.4	5.3	**11.9**
2013	4.7	9.3	7.4	12.7	6.8	15.1	3.9	14.8	**22.8**
2014	4.6	9.1	6.8	11.7	6.5	14.4	3.9	15.1	**21.9**
2015	16.0	31.5	18.3	31.4	15.1	33.5	10.0	38.4	**59.5**
Total	**51.0**	**100.0**	**58.2**	**100.0**	**45.2**	**100.0**	**26.1**	**100.0**	**180.5**

1.10 Calculation of weights-of-evidence
1.10.1 *A priori* probabilities of fire events

The weights-of-evidence originated from the Bayesian method of calculating conditional probabilities. Its application in modeling the dynamics of land-use and land-cover change assumes that it is possible to calculate the probability *a posteriori* of an event happening based on information obtained *a priori* from a set of conditions (evidence) that favored or determined the event in question. In our study, a set of conditions or "evidences" was transformed into maps of distance variables (maps of continuous variables) and maps of categorical variables (maps of classes) to represent influences on the occurrence of forest fires in the study area in 2015/2016 (Figure S4). The calculations of the weights-of-evidence and of the probability map were carried out in a sub-model in the Dinamica-EGO software with a stacking of the maps (Soares-Filho et al., 2014) (Figures S5 and S6).
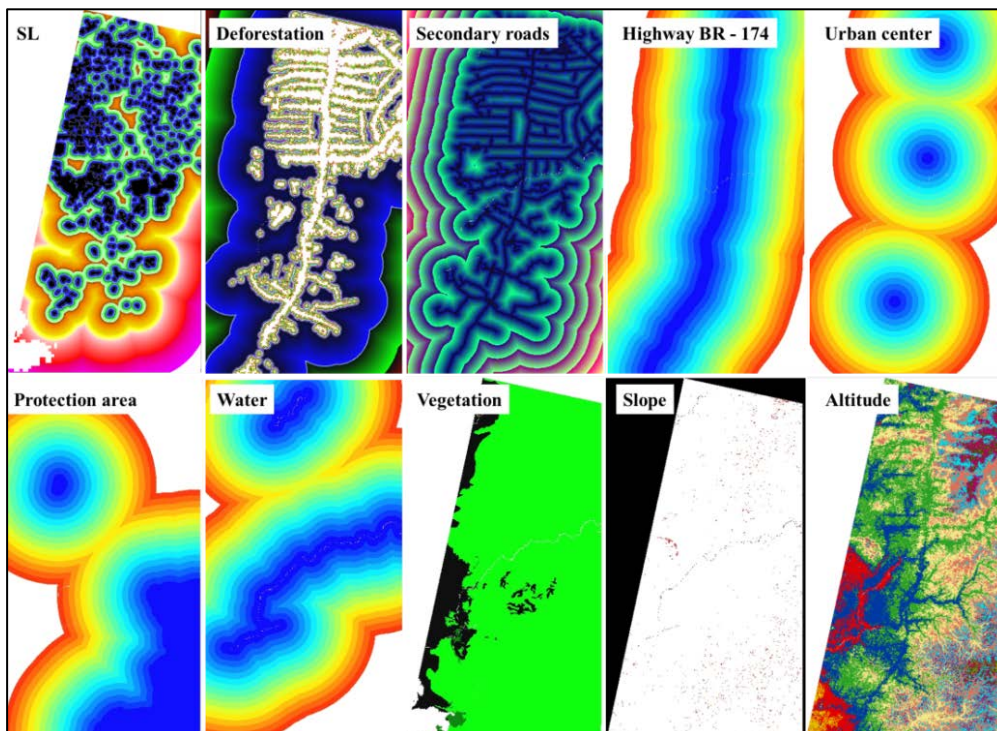
Figure S4. Set of continuous variables (with distance ranges) and categorical variables (vegetation, slope and altitude). SL = selective logging.
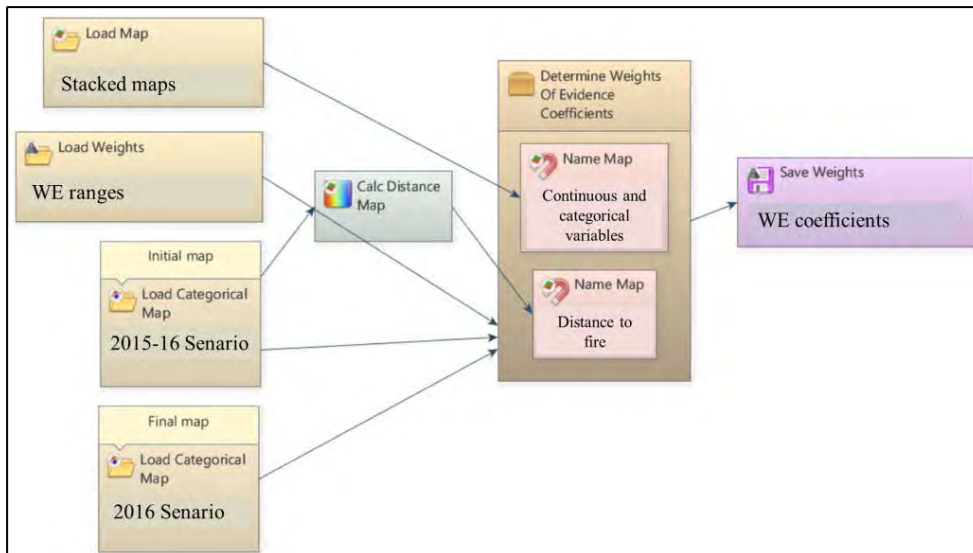
Figure S5. Submodel of the Dinamica-EGO software for calculating the weights-of-evidence coefficients. **Source**: adapted of the Dinamica-EGO guidebook (https://csr.ufmg.br/dinamica/).
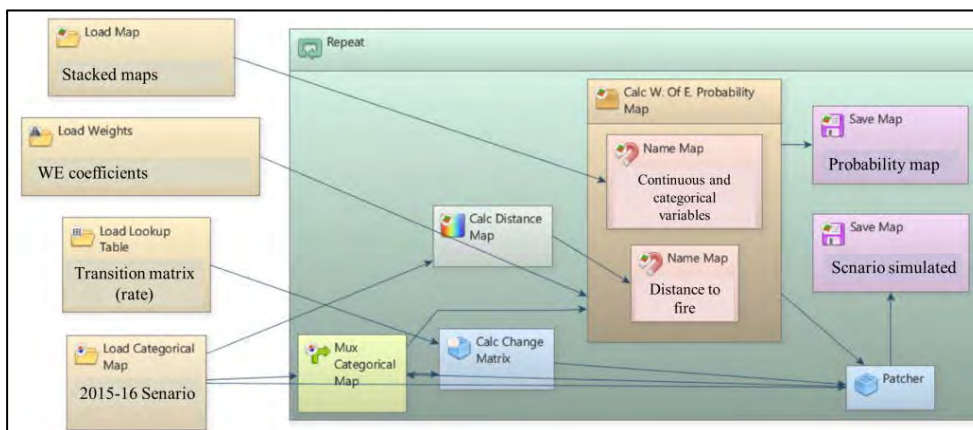
Figure S6. Submodel of the Dinamica-EGO software for calculating the map of transition probabilities and the simulated fire map. **Source**: adapted of the Dinamica-EGO guidebook (https://csr.ufmg.br/dinamica/).

The influence of the weights-of-evidence can be positive or negative. The coefficients of the weights-of-evidence are positive when they favor or promote an increase in the probability of a class transition, and they are negative when they inhibit the class transition, decreasing its probability of occurrence. For example, the spatial probability map (derived from weights-of-evidence) will indicate to the software which sets of pixels representing forest on a land-use map at time t_1 have a greater chance or probability of changing to a burnt area at time t_2. The variable "distance to secondary roads," for example, will have its maximum positive (+) weight-of-evidence in the first meters away from the fire, and at progressively greater distances this influence will decrease until it becomes negative (-), reaching its negative maximum at the most distant point.

In the modeling the weights-of-evidence represent the amount of influence of each variable on the probability of transition of a cell representing a particular state (i: forest) to change to another state (j: fire (F)), depending, for example, on its location within a distance range. In this way, the cell that is located closest to where the phenomenon occurred has a higher chance or greater probability. This relationship can be represented by equations (1) to (9) below, derived from the Bayesian inference method:

$$P(F/A) = \frac{P(F \cap A)}{P(A)} \tag{1}$$

$$P(A/F) = \frac{P(A \cap F)}{P(F)} \tag{2}$$

$$P(A \cap F) = P(A/F) * P(F) \tag{3}$$

Likewise, considering non-event F, as not F ($\hat{F}$), we obtain (4):

$$P(\hat{F}/A) = P(\hat{F}) * \frac{P(A/\hat{F})}{P(A)} \tag{4}$$

Now replacing (4) in (1), we have (5):

$$P(F/A) = P(F) * \frac{P(A/F)}{P(A)} \tag{5}$$

Applying the ratio between Equations (6) and (7), we obtain (8): (6)

$$O(F/A) = O(F) * \frac{P(A/F)}{P(A/\hat{F})} \tag{6}$$

$$\log O(F/A) = \log O(F) + \log \frac{P(A/F)}{P(A/\hat{F})} \tag{7}$$

$$\log O(F/A) = \log O(F) + W^+ \tag{8}$$

Thus:

$$\log O(F/A) = \log O(F) + \sum_{i=1}^{n} W_i^+ \tag{9}$$

Where "{F}" and "O {F / A}" are proportions of *a priori* probability that the "F" (fire) event occurs, and the fire event occurs given a spatial pattern "A", respectively. "W +" is, therefore, the weight-of-evidence of event F occurring given the spatial pattern "A". Thus, the calculation of the *a posteriori* spatial transition probability "i → j" for a spatial data set "(B, C, D, ... N)" can be represented by (10):

$$P(i \rightarrow j/B \cap C \cap D ... \cap N) = \frac{e^{\sum W_i^+}}{1 + e^{\sum W_i^+}} \tag{10}$$

Where, "B, C, D, ..., N" are values of the k spatial variables estimated at positions "x, y", being represented by their respective weights-of-evidence "W + N". For more details on the weights-evidence method, see Barni et al. (2015).

1.10.2 Correlation between spatial variables in the calculation of weights-of-evidence
Application of the weights-of-evidence method presupposes spatial independence between variables. In the case of pairs of variables with a correlation above 0.5, one of them must be removed from the set of maps that will be used in the modeling in order to guarantee compliance with the model's assumption of independence (Bonham-Carter, 1994). This independence is

measured or estimated by observing some parameters, mainly that of contingency, which, like Pearson's correlation analysis (Figueiredo-Filho and Silva Junior, 2009), indicates the amount of correlation that exists between two spatial variables (Table S10).

Table S10. Correlated variables in the calculation of the weights of evidence.

Variable 1	Variable 2	CHI Sq.	CRAMMER	CONTING	ENTROPY	INF_C*INCERT
Deforestation	Secondary roads	26324385.8	0.38	0.86	4.36	0.35
Fire	Deforestation	13591362.2	0.31	0.81	4.97	0.20
SL	Secondary roads	11137374.0	0.30	0.78	4.75	0.21
BR-174	Village	12300562.7	0.29	0.78	4.74	0.24
Fire	SL	10654858.5	0.26	0.77	5.07	0.18
Fire	Secondary roads	10387346.3	0.29	0.77	5.04	0.18
Deforestation	SL	9312302.5	0.26	0.75	4.87	0.17
BR-174	Secondary roads	7309303.3	0.22	0.68	4.88	0.14
BR-174	Deforestation	7117818.5	0.21	0.67	4.88	0.14
Fire	Protected area	4585235.4	0.20	0.65	5.02	0.13
Fire	BR-174	5084155.0	0.20	0.65	5.22	0.09
Protected area	SL	4263722.4	0.19	0.64	4.83	0.13
Protected area	BR-174	4550167.7	0.19	0.63	4.80	0.13
Secondary roads	Village	4673617.7	0.19	0.61	5.07	0.11
Deforestation	Village	4629794.4	0.18	0.61	5.09	0.10
BR-174	SL	3819157.9	0.17	0.59	5.06	0.07
Protected area	Altitude	3321756.0	0.23	0.59	4.28	0.12
Fire	Village	3152213.0	0.14	0.57	5.35	0.07
SL	Water	2948194.9	0.15	0.56	5.14	0.06
Protected area	Secondary roads	3536961.0	0.16	0.56	4.90	0.09
Protected area	Deforestation	3378198.9	0.15	0.55	4.93	0.09
Protected area	Village	2480305.7	0.14	0.53	5.06	0.07
Protected area	Water	2553570.6	0.14	0.52	4.96	0.08
Water	Altitude	2382190.2	0.19	0.52	4.64	0.07
Altitude	Vegetation	2335823.6	0.40	0.49	2.34	0.10
Secondary roads	Altitude	2291973.7	0.18	0.49	4.60	0.06
SL	Village	2019896.1	0.12	0.48	5.23	0.06
Water	SL year class	214633.3	0.21	0.48	4.20	0.06
Village	SL year class	211868.6	0.21	0.48	4.30	0.06
Protected area	SL year class	181646.8	0.20	0.47	4.06	0.08
BR-174	Altitude	1947197.2	0.17	0.46	4.58	0.06
Fire	Water	1609818.9	0.10	0.45	5.42	0.04
Deforestation	Water	2167922.4	0.11	0.45	5.25	0.05
Deforestation	Altitude	1804270.1	0.16	0.44	4.61	0.05
BR-174	SL year class	168417.7	0.18	0.44	4.18	0.05
Fire	Altitude	1596435.5	0.15	0.43	4.85	0.04
SL	Altitude	1589559.1	0.15	0.42	4.64	0.04
BR-174	Water	1463864.6	0.10	0.40	5.25	0.03
Fire	SL year class	133323.5	0.16	0.40	4.38	0.05
Village	Altitude	1239948.2	0.13	0.39	4.74	0.04
Water	Secondary roads	1464261.7	0.10	0.38	5.29	0.04
Deforestation	SL year class	111350.3	0.15	0.37	4.21	0.04
Water	Village	1102794.6	0.07	0.36	5.38	0.03
Water	Vegetation	771589.5	0.25	0.33	3.11	0.04

BR-174	Vegetation	798968.3	0.24	0.32	2.98	0.04
Slope	Altitude	838470.5	0.11	0.32	4.11	0.03
Protected area	Vegetation	654567.6	0.23	0.31	2.79	0.03
Secondary roads	SL year class	68851.5	0.12	0.30	3.87	0.02
SL year class	Altitude	68036.6	0.12	0.29	3.69	0.03
Secondary roads	Vegetation	475077.7	0.18	0.25	3.01	0.02
Village	Vegetation	440054.3	0.18	0.25	3.13	0.02
SL	Vegetation	444832.3	0.18	0.24	3.05	0.02
Deforestation	Vegetation	327915.6	0.15	0.21	3.00	0.02
Fire	Vegetation	323501.9	0.15	0.21	3.26	0.01
SL year class	Vegetation	26428.0	0.14	0.19	2.18	0.02
Protected area	Slope	221586.4	0.06	0.18	4.52	0.01
Water	Slope	203287.6	0.06	0.17	4.76	0.01
SL	Slope	154153.7	0.05	0.14	4.74	0.00
Secondary roads	Slope	145011.5	0.05	0.14	4.69	0.00
Deforestation	Slope	128456.0	0.04	0.13	4.68	0.00
BR-174	Slope	123456.6	0.04	0.13	4.66	0.00
Fire	Slope	91464.5	0.04	0.11	4.94	0.00
Slope	Vegetation	54819.5	0.06	0.09	2.46	0.00
Village	Slope	29033.2	0.02	0.06	4.80	0.00
SL year class	Slope	2855.3	0.02	0.06	3.98	0.00
SL	SL year class	0.0	0.00	0.00	1.93	0.00

SL = Selective logging

1.11 Model validation using an exponential decay function and fuzzy similarity

The "Calc reciprocal similarity map" function in Dinamica-EGO calculates a two-way similarity from the first map (simulated scenario) to the second (initial scenario) and from the second to the third (final scenario) (Figure S7). It is advisable to always chose the smaller similarity value since random maps tend to produce artificially high fits when compared univocally, because they spread the changes over the entire map. This test employs an exponential decay function truncated outside of a window size of 11×11 cells. The test result is returned in a .csv table file (Figure S8).
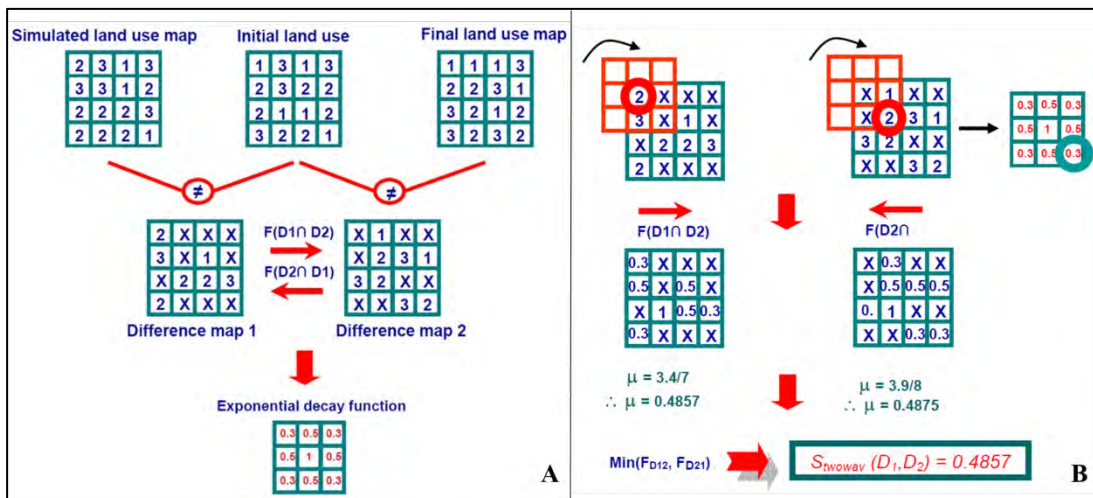
Figure S7. Fuzzy comparison method using a map of differences and an exponential decay function. The process applies a constant decay function in which all window weights are set to 1 (**A**). The window convolutes over the map, obtaining a fuzzy value for the central cell (**B**). X = null values in the map. **Source**: adapted from the Dinamica-EGO guidebook (https://csr.ufmg.br/dinamica/).
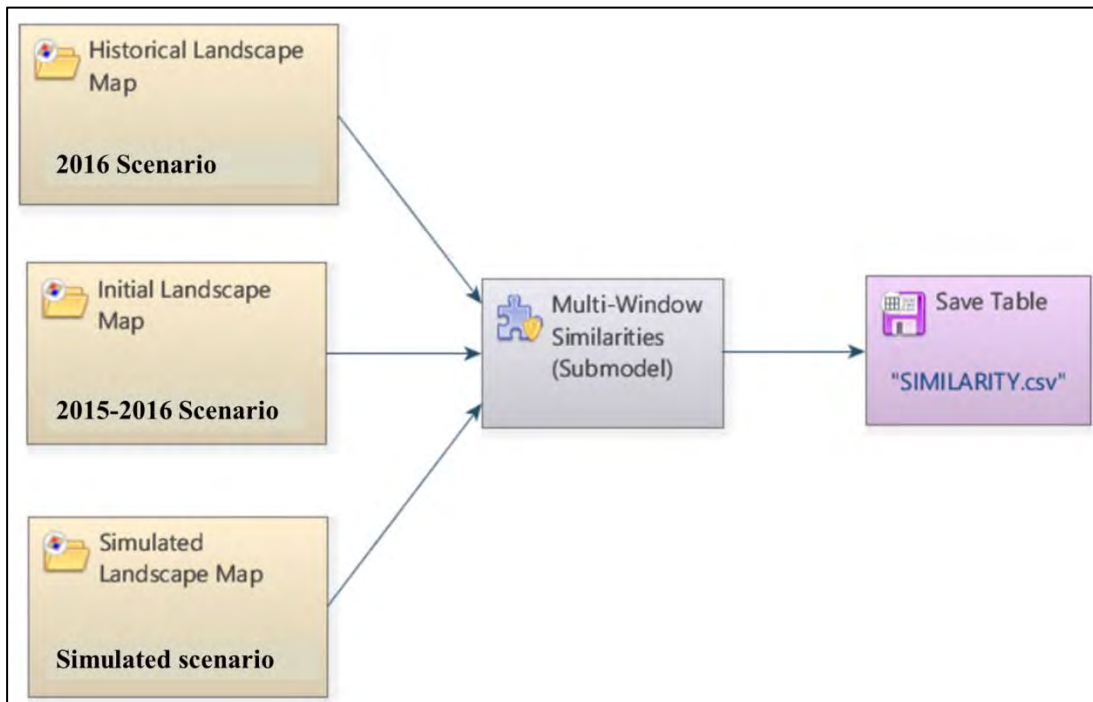
Figure S8. Submodel for similarity calculation in Dinamica-EGO software. **Source**: adapted from the Dinamica-EGO guidebook (https://csr.ufmg.br/dinamica/).

2. Results
2.1 Areas of occurrence

The areas of occurrence of the main variables distributed in the study area are presented in Table S11. The original forest area was estimated at 6512.4 km^2, representing 97.8% of the study area.

Table S11. Original forest area (km^2), protected areas, non-forest and deforestation occurring in the study area.

	Class	Area (km^2)	%	Forest fire (km^2)	Forest fire % of forest area	SL-fire (km^2)	SL-fire % of forest fire area	SL (km^2)	SL-fire (%) of SL area
Original vegetation	**Forest**	6,512.4	97.8						
	Non-forest	144.9	2.2						
	Total	**6,657.3**	**100.0**						
2016 vegetation	**Forest**	5,410.3	81.3	682.2	12.6	180.7	26.5	644.8	28.0
	Deforestation	1,102.1	16.6	–	–	–	–	–	–
	Non-forest	144.9	2.2	–	–	–	–	–	–
	Total	**6,657.3**	**100.0**						
Protected areas	**Indigenous land**	875.6	13.2	0.0	0.0	–	–	–	–
	Anauá National Forest	2.6	0.04	2.0	76.9	–	–	–	–

2.2 Estimates of biomass by forest type

Dense ombrophilous forest was the most affected by understory fires, totaling 532.7 km^2 and the estimated affected dry biomass at the time of the fire totaling 26.2×10^6 Mg. Ecotone forest had the smallest area (9.3 km^2) and the smallest amount (0.3×10^6 Mg) of affected biomass (Table S12).

Table S12. Estimated biomass before and after logging in the area affected by fire separated by forest type and by selective-logging status.

Forest	Original biomass (prior to logging)				Affected biomass (biomass at time of fire)						
	Total area affected by fire (km^2)	Total biomass in area affected by fire (10^6 Mg)	% of total biomass in area affected by fire	Mean original biomass (Mg ha^{-1})	Area W/SL (km^2)	Biomass after logging (10^6 Mg)	Biomass removed or killed by SL (10^6 Mg)	Affected biomass in area with SL (10^6 Mg)	Area Wo/SL (km^2)	Affected biomass in area Wo/SL (10^6 Mg)
Campinarana	140.0	3.6	13.2	255.6	28.3	0.71	0.1	0.7	111.7	2.9
Ecotone	9.3	0.33	1.2	360.3	0.0	0.0	0.0	0.0	9.3	0.3
Ombrophilous	532.7	23.2	85.6	435.3	152.3	6.63	0.5	6.1	380.3	16.6
Total	**681.9**	**27.1**	**100**	**397.4**	**180.62**	**7.34**	**0.6**	**6.7**	**501.3**	**19.8**

The estimation of forest biomass was performed for each forest type separately for areas with and without selective logging (SL). The dense ombrophilous forest (Ds) had the largest extension in terms of occupied area (87.8%) and in terms of biomass (92.5%) in relation to the total biomass (277.37×10^6 Mg) estimated for the original forest areas. The biomass of the areas under SL (27.6×10^6 Mg) represented 9.9% of the total biomass found in the study area, and 95.3% of that biomass was under dense ombrophilous forest (Table S13).

Table S13. Estimated biomass (Mg) in the study area separated by areas affected by selective logging (SL) (W-SL) and areas not affected by SL (Wo-SL).

Type	Area (km^2)	%	Biomass (10^6 Mg)	Mean (Mg ha^{-1})	Wo/SL 10^6 Mg	%	W/SL (10^6 Mg)	%
Campinarana	727.9	11.2	18.7	256.3	17.4	93.0	1.30	7.0
Ecotone	63.7	1.0	2.1	335.5	2.1	99.1	0.02	0.9
Ombrophilous	5,720.8	87.8	256.7	448.5	230.3	89.7	26.3	10.3
Total	**6,512.4**	**100.0**	**277.4**	**425.9**	**249.8**	**90.0**	**27.6**	**9.9**

Wo/SL = without selective logging. W-SL = with selective logging.

The cumulative loss of original biomass by deforestation up to 2016 was estimated at 48.04×10^6 Mg, representing more than twice (2.1 times) the biomass affected by SL in our study area. The area deforested in dense ombrophilous forest (1059.3 km^2) represented 96.1% of the total area deforested by 2016 and 97.5% of the total biomass lost (Table S14).

Table S14. Biomass lost due to cumulative deforestation up to 2016.

Deforestation	Area (km^2)	%	Biomass (10^6 Mg)	%	Mean (Mg ha^{-1})
Campinarana	33.8	3.1	0.9	1.8	255.6
Ecotone	8.8	0.8	0.3	0.7	367.4
Ombrophilous	1,059.3	96.1	46.9	97.5	442.3
Total	**1,101.9**	**100.0**	**48.0**	**100.0**	**436.0**

2.3 Vulnerability of the forest to understory fires in SL areas

SL influenced the spread of fire in the study area during the 2015/2016 El Niño event within the fire-severity classes. Based on NDVI image analyses, the graphs in Figure S9 show positive correlations between fires and the logging practiced in years immediately prior to the fires.
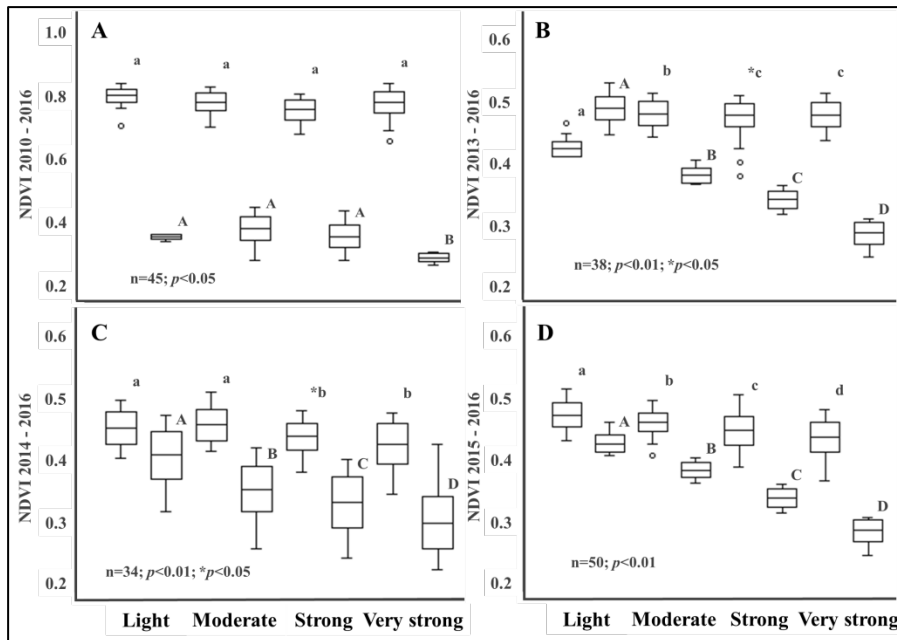
Figure S9. Comparison between NDVI values in SL areas in years prior to the fires with the NDVI values in the fire image for 2016. (A) Comparison of NDVI values between the years 2010 and 2016. (B) Comparison of NDVI values between the years 2013 and 2016. (C) Comparison of NDVI values between the years 2014 and 2016 and (D) comparison of NDVI values between the years 2015 and 2016. The lower-case letters above the boxes indicate statistical results between the NDVI values in years prior to the fires considering the fire-severity classes of the fires, while upper-case letters indicate the statistical results for the NDVI values in the 2016 image at the fire-event locations, also considering the severity classes.

2.4 Fire and SL behavior as a function of forest-edge distance

The highest occurrence of forest fires (114.9 km^2: 20.1%) in the study area was found in the range between 0 to 120 m from the forest edge. The SL presented a similar result reaching 113.9 km^2 (24.3%) in the first interval. The burned areas affected by SL were calculated at 161.2 km^2 in the range between 0 and 1200 m, representing 89.4% of the total reached in the study area (Table S15).

Table S15. Fire and SL occurrence depending on the distance from the forest edge.

Range (m)	Fire (km^2)	%	SL (km^2)	%	SL x Fire (km^2)	%	SL / Fire (%)	SL x Fire / Fire (%)	SL x Fire / SL (%)
0 -- 120	114.9	20.1	113.9	24.3	23.7	14.7	99.1	20.6	20.8
120 -- 240	95.3	16.7	58.2	12.4	25.3	15.7	61.1	26.5	43.4
240 -- 360	77.8	13.6	55.2	11.8	23.5	14.6	70.9	30.2	42.5
360 -- 480	68.8	12.0	52.8	11.3	21.2	13.2	76.7	30.9	40.2
480 -- 600	55.6	9.7	47.5	10.1	17.9	11.1	85.3	32.2	37.7
600 -- 720	43.6	7.6	38.1	8.1	14.1	8.7	87.2	32.3	37.0
720 -- 840	37.8	6.6	32.5	6.9	11.8	7.3	85.9	31.2	36.3
840 -- 960	31.7	5.6	28.4	6.1	9.9	6.1	89.5	31.0	34.7
960 -- 1080	25.3	4.4	23.0	4.9	7.7	4.7	91.2	30.3	33.2
1080 -- 1200	21.0	3.7	19.3	4.1	6.3	3.9	92.2	30.1	32.7
Total	**571.7**	**100.0**	**468.8**	**100.0**	**161.2**	**100.0**			
Percent	**682.2**	**83.8**	**644.8**	**72.7**	**180.4**	**89.4**			

2.5 Model-validation results

The results of the validation test are shown in Figure S10. The model containing all variables showed the greatest similarity between the observed and simulated scenarios.
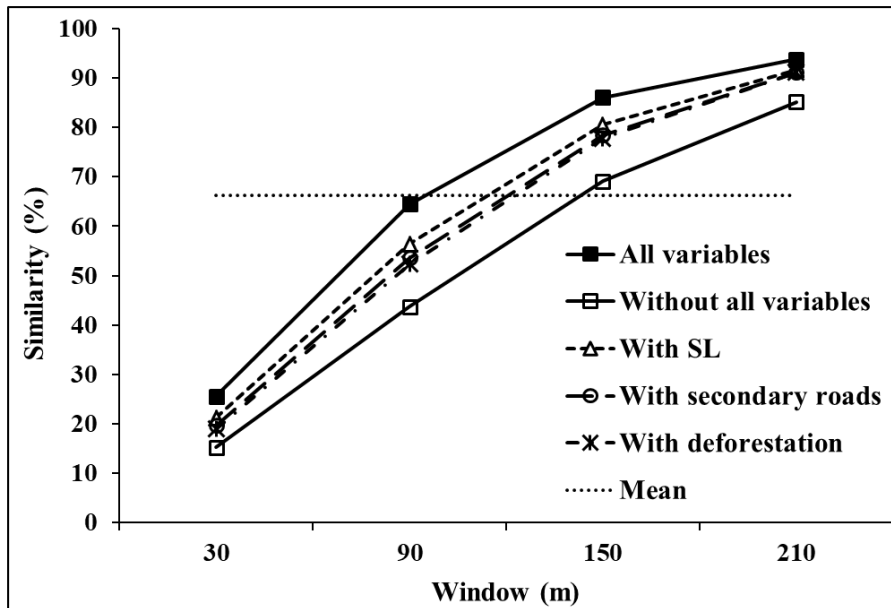
Figure S10. Similarity test between the modeled maps and the fire map for 2016.

2.6 Forest vulnerability to fire

The assessment of the vulnerability maps showed that the SL influenced the spread of fire in the study area during the 2015/2016 El Niño event. The exposure of forest areas to fires increased by 366.2% in the most-vulnerable range, which ranged from 79.11 to 99.99% (0.7911 to 0.9999 probability), with the presence of SL areas in the model compared to the absence of SL in the model (Table S16; Figures S11 and S12).

Table S16. Classes of vulnerability of the forest to forest fires.

Range	Whole area regardless of impacts Area (km²)	%	Without SL Area (km²)	%	Without secondary roads Area (km²)	%	Without deforestation Area (km²)	%
0.0004 - 0.1488	2,550.4	47.1	1,750.1	32.3	2,467.7	45.6	2,478.5	45.8
0.1489 - 0.3955	421.4	7.8	822.4	15.2	511.3	9.4	501.1	9.3
0.3956 - 0.6109	407.5	7.5	938.9	17.3	500.3	9.2	478.1	8.8
0.6110 - 0.7910	547.7	10.1	1,315.5	24.3	588.7	10.9	609.0	11.2
0.7911 - 0.9999	1,487.9	27.5	587.9	10.9	1,346.7	24.9	1,348.1	24.9
Total	**5,414.8**	**100.0**	**5,414.8**	**100.0**	**5,414.8**	**100.0**	**5,414.8**	100.0
Range	Without SL, roads or deforestation Area (km²)	%	With SL Area (km²)	%	With secondary roads Area (km²)	%	With deforestation Area (km²)	%
0.0004 - 0.1488	1,576.3	29.1	1,859.3	34.3	1,557.9	28.8	1,497.2	27.7
0.1488 - 0.3955	784.3	14.5	821.7	15.2	966.9	17.9	985.9	18.2
0.3956 - 0.6109	694.7	12.8	671.2	12.4	707.8	13.1	802.0	14.8
0.6110 - 0.7910	2,045.3	37.8	912.2	16.8	735.8	13.6	951.1	17.6
0.7911 - 0.9999	314.2	5.8	1,150.4	21.2	1,446.4	26.7	1,178.6	21.8
Total	**5,414.8**	**100.0**	**5,414.8**	**100.0**	**5,414.8**	**99.9**	**5,414.8**	100.0
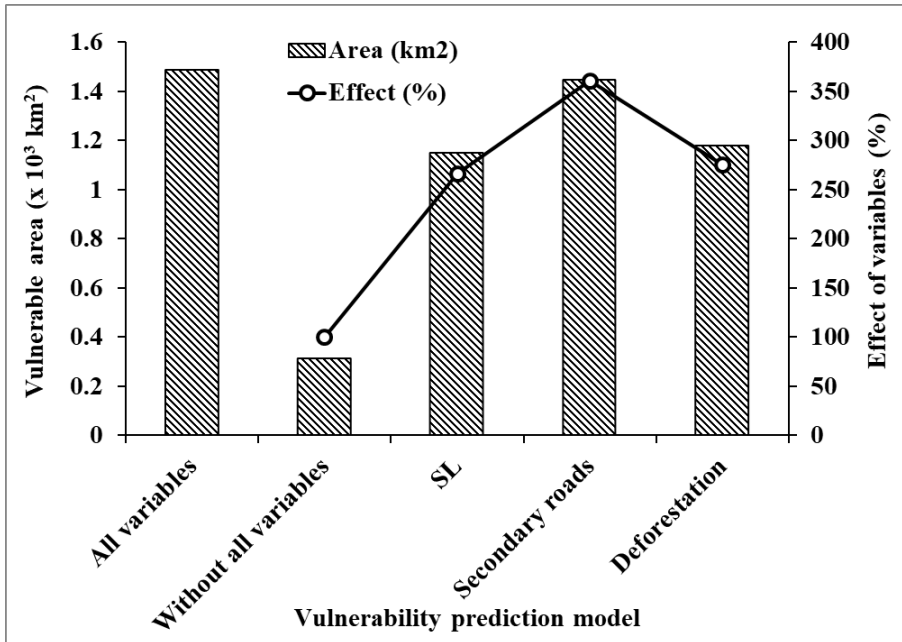
Figure S11. Area vulnerable to understory forest fires in the study area.
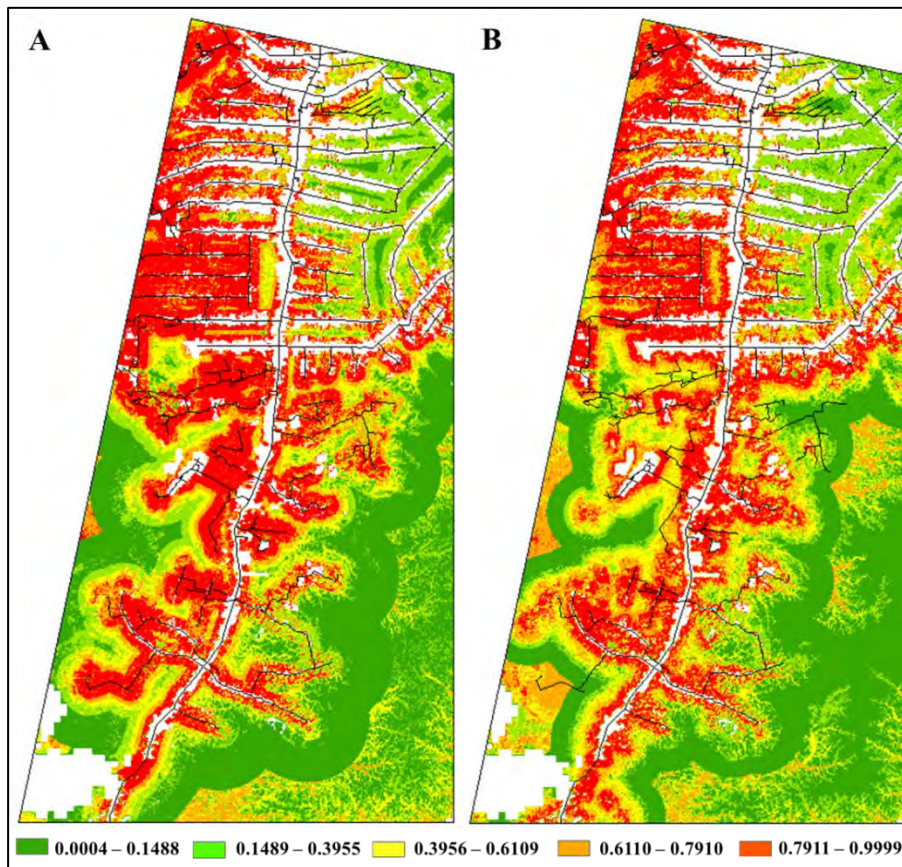
Figure S12. Maps of the vulnerability of the forest to understory fires. (A) forest-vulnerability map calculated from variables not correlated with "secondary roads," plus the "secondary roads" variable and (B) forest-vulnerability map calculated from variables not correlated with "deforestation," plus the "deforestation" variable. The legend below the figure shows the ranges of probability ([0.1]) of the forest being affected by fire.
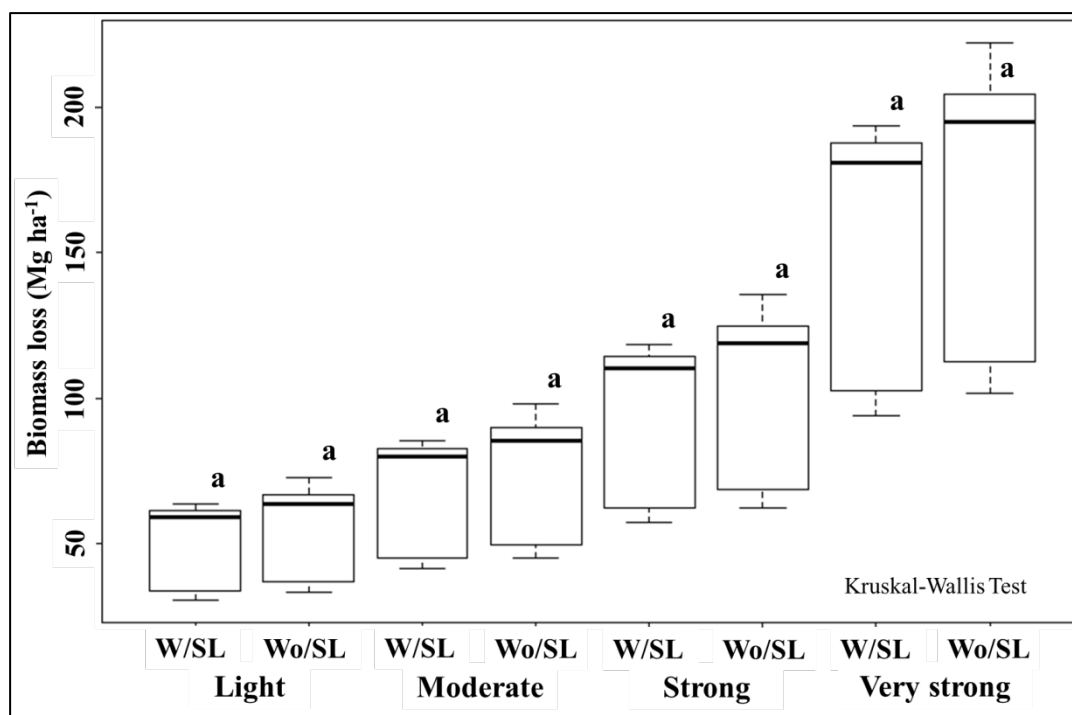
Figure S-13. Biomass loss (Mg ha^{-1}) by fire-severity class in areas with SL (W/SL) and areas without SL (Wo/SL) considering all forest types in the study area. The lower-case letters above the boxes indicate that there was no significant difference ($p < 0.05$) between the loss of biomass by fire in previously logged areas and unlogged areas within each severity class.

References

Barni, P.E., Fearnside, P.M., Graça, P.M.L.A., 2015. Simulating deforestation and carbon loss in Amazonia: impacts in Brazil's Roraima state from reconstructing Highway BR-319 (Manaus-Porto Velho). Environmental Management, 55, 124–1138. http://rd.springer.com/article/10.1007%2Fs00267-015-0447-7

Barni, P.E., Silva, E.B.R., Silva, F.C.F., 2017. Incêndios florestais de sub-bosque na zona de florestas úmidas do sul de Roraima: Área atingida e biomassa morta. In: Anais do Simpósio Brasileiro de Sensoriamento Remoto 2017. Campinas, SP, Brazil: Galoá, pp. 6280-6287. Available at: https://bityl.co/5JeV. Accessed on: 21 November 2020.

Bonham-Carter, G., 1994. Geographic Information Systems for Geoscientists: Modeling with GIS. Pergamon, New York, USA. 398 pp.

Brazil, IBGE (Instituto Brasileiro de Geografia e Estatística), 2021. Produção da Extração Vegetal e da Silvicultura: Tabela289. Available at: https://sidra.ibge.gov.br/Tabela/289. Accessed on: 19 March 2021.

Brazil, INPE (Instituto Nacional de Pesquisas Espaciais), 2020. Projeto PRODES – Monitoramento da Floresta Amazônica por Satélite. São José dos Campos, SP, Brazil: INPE. Available at: https://bityl.co/5JeS. Accessed on: 21November 2020.

da Silva, R.P., 2007. Alometria, Estoque e Dinâmica da Biomassa de Florestas Primárias e Secundárias na Região de Manaus (AM). Ph.D. Thesis in tropical forest science, Instituto Nacional de Pesquisas da Amazônia (INPA), Manaus, Amazonas, Brazil. https://repositorio.inpa.gov.br/bitstream/1/4966/1/Roseana_Silva.pdf

Fearnside, P.M., 1995. Global warming response options in Brazil's forest sector: Comparison of project-level costs and benefits. Biomass and Bioenergy, 8(5), 309-322. https://doi.org/10.1016/0961-9534(95)00024-0

Fearnside, P.M., 1997. Wood density for estimating forest biomass in Brazilian Amazonia. Forest Ecology and Management, 90(1), 59-89. https://doi.org/10.1016/S0378-1127(96)03840-6

Figueiredo Filho, D.B., Silva Junior, J.A., 2009. Desvendando os mistérios do coeficiente de correlação de Pearson (r). Política Hoje, 18(1), 115-146. https://periodicos.ufpe.br/revistas/politicahoje/article/view/3852/3156

Higuchi, N., Santos, J., Ribeiro, R.J., Minette L., Biot, Y., 1998. Biomassa da parte aérea da vegetação da floresta tropical úmida de terra-firme da Amazônia brasileira. Acta Amazonica, 28(2), 153-166. https://doi.org/10.1590/1809-43921998282166

Nogueira, E.M., Nelson, B.W., Fearnside, P.M., 2005. Wood density in dense forest in central Amazonia, Brazil. Forest Ecology and Management, 208(1-3), 261-286. https://doi.org/10.1016/j.foreco.2004.12.007

Nogueira, E.M., Fearnside, P.M., Nelson, B.W., Barbosa, R.I., Keizer, E.W.H., 2008. Estimates of forest biomass in the Brazilian Amazon: New allometric equations and adjustments to biomass from wood-volume inventories. Forest Ecology and Management, 256(11), 1853-1857. https://doi.org/10.1016/j.foreco.2008.07.022

Saldarriaga, J.G., West, D.C., Tharp, M., Uhl, C., 1988. Long-term chronosequence of forest succession in the upper Rio Negro of Colombia and Venezuela. Journal of Ecology,76, 938–958. https://doi.org/10.2307/2260625

Silveira, L.H.C., Rezende, A.V., Vale, A.T., 2013. Teor de umidade e densidade básica da madeira de nove espécies comerciais amazônicas. Acta Amazonica, 43(2), 179–184. https://doi.org/10.1590/S0044-59672013000200007

Soares-Filho, B.S., Ferreira, B.M., Filgueira, D.S., Rodrigues, H.O., Hissa, L.B.V., Lima, L.S., Machado, R.F., Costa, W.L.S., 2014. Dinamica project. Remote Sensing Center. Federal University of Minas Gerais (UFMG), Belo Horizonte, Minas Gerais, Brazil. Available at: http://www.csr.ufmg.br/dinamica/. Last access: 12 June 2020.